EFFECTS OF HUMIDITY ON MECHANICAL PROPERTIES AND MICROSTRUCTURE OF 3D PRINTED PLA FILAMENT

This report is submitted in accordance with requirement of the Universiti Teknikal Malaysia Melaka (UTeM) for Bachelor Degree of Manufacturing Engineering (Hons.)

by

FATIMA HANIM BINTI HAMEZAH

FACULTY OF MANUFACTURING ENGINEERING

2021

DECLARATION

I hereby, declared this report entitled “Effects of Humidity on Mechanical Properties and Microstructure of 3D Printed PLA Filament” is the result of my own research except as cited in references.

Signature : ……

Author’s Name : FATIMA HANIM BINTI HAMEZAH

Date : 2 September 2021

APPROVAL

This report is submitted to the Faculty of Manufacturing Engineering of Universiti Teknikal Malaysia Melaka as a partial fulfilment of the requirement for Degree of Manufacturing Engineering (Hons). The member of the supervisory committee is as follow:

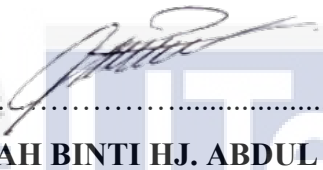

……

(DR. RAHIMAH BINTI HJ. ABDUL HAMID)

DR. RAHIMAH BINTI HJ. ABDUL HAMID
Senior Lecturer
Faculty of Manufacturing Engineering
Universiti Teknikal Malaysia Melaka
Hang Tuah Jaya
76100 Durian Tunggal, Melaka

ABSTRAK

Filamen asid polilaktik (PLA) sensitif terhadap kelembapan kerana sifat higroskopiknya menyebabkan gelembung dan kualiti cetakan yang kurang baik. Ramai pengguna Fused Deposition Modelling (FDM) mengabaikan kawalan kelembapan dan cara penyimpanan filamen yang betul selepas digunakan. Banyak kajian memberi tumpuan kepada kesan parameter proses pada bahagian cetakan 3D; tetapi pengaruh kelembapan pada kualiti percetakan kurang diterokai. Kelembapan boleh mempengaruhi sifat-sifat mekanikal bahagian cetakan 3D kerana kewujudan air boleh mengubah ikatan rantai polimer justeru melemahkan kekuatan mekanikal. Objektif kajian ini adalah untuk mengkajit pengaruh kelembapan pada kekuatan tegangan dan lenturan serta perubahan mikrostruktur. Oleh itu, tiga tetapan bersyarat telah dihasilkan; menggunakan gulungan PLA baru sebagai rujukan, gulungan PLA yang disimpan dalam beg vakum bersama agen pengering, dan gulungan PLA yang disimpan dalam persekitaran terbuka, terdedah kepada kelembapan selama 24 - 150 jam. Filamen ini digunakan untuk menghasilkan spesimen yang mematuhi ASTM D638 – Jenis IV (spesimen tegangan) dan ASTM D790 (spesimen lenturan) untuk diuji pada Mesin Ujian Universal Shimadzu AGS-X (UTM) pada kelajuan 5mm/s, dan 50 mm/s. Spesimen tegangan yang telah patah kemudiannya disalut dan digunakan pada mesin Scaning Electron Microscope (SEM) untuk mengkaji mikrostrukturnya. Keputusan menunjukkan bahawa kelembapan mengurangkan kekuatan tegangan dan lenturan sambil meningkatkan keupayaan untuk patah. Kehadiran kelembapan memplastikkan polimer, memudahkannya untuk dibentuk dan mengurangkan ketegarannya kerana kelembapan mengubah struktur molekul polimer. Imej SEM menunjukkan bahawa kelembapan memperluaskan jurang interlayer, menggalakkan peningkatan dalam keupayaan untuk patah disebabkan oleh peningkatan ruang pengubahsuaian makromolekul. Namun, kami mendapati bahawa filamen terpakai yang disimpan dalam beg vakum bersama beberapa agen pengering menunjukkan kekuatan tegangan yang setara dengan spesimen rujukan. Kesimpulannya, kelembapan mempengaruhi sifat-sifat mekanikal dan harus dikawal untuk kualiti percetakan bahagian PLA yang baik. Sebagai cadangan, semua pengguna percetakan 3D dinasihatkan untuk menyimpan filamen PLA mereka dalam beg vakum bersama agen pengering untuk menggantikan kabinet pengeringan bagi mengawal kelembapan dalam percetakan.

ABSTRACT

Polylactic acid (PLA) filament is sensitive to humidity due to its hygroscopic properties, resulting in bubbles and poor printing quality of 3D printed parts. Even though it is significant to control the PLA filament's humidity and store it properly after use, many Fused Deposition Modelling (FDM) users ignore this factor. Many studies focus on the effect of process parameters on the 3D printed part; however, the influence of humidity on the printing quality is less explored. Moisture can influence the mechanical properties of 3D printed parts due to the water's existence, which could alter the polymer chain's bonding, resulting in a lower mechanical strength. The objectives of this study are to investigate the influence of humidity on the tensile strength, fracture strength, and the alteration of microstructure caused by moisture. In order to do so, three conditional settings were established; a new PLA roll acts as the reference, used PLA roll stored in the vacuum bag with desiccant, and used PLA roll stored in an open environment, exposed with the humidifier for 24 - 150 hours. These filaments are subsequently used to fabricate specimens that comply with ASTM D638 – Type IV (tensile specimen) and ASTM D790 (flexural specimen) to be tested in the Shimadzu AGS-X Universal Testing Machine (UTM) at the speed of 5mm/s, and 50 mm/s, respectively. The fractured tensile specimen is then sputter-coated and used in the Scanning Electron Microscope (SEM) machine to study its microstructure. The results show that the humidity decreases the tensile and flexural strength while increasing the fracture strain. The presence of moisture causes the polymer to plasticize, increasing its deformability and reducing its rigidity as the moisture alters its molecular structure. The SEM images show that humidity expands the interlayer gap, promoting enhancement in the fracture strain due to increased macromolecules deformation space. Nevertheless, we found that the used PLA filament stored in a vacuum bag with some desiccants shows an equivalent tensile strength with the reference specimen. To conclude, humidity influences the mechanical properties and should be controlled for a good printing quality of PLA parts. As a recommendation, all 3D printing users are advised to store their PLA filament in a vacuum bag with dehumidifying agents to substitute for the drying cabinet to control the humidity in their printing.

DEDICATION

This humble work is dedicated to my beloved father, mother and siblings.

ACKNOWLEDGEMENT

Praises and thanks to Allah, the most gracious and the most merciful, for His countless of blessings throughout my journey to complete this final year project successfully.

I would like to express my deep and sincere gratitude to my supervisor, Dr. Rahimah Binti Hj. Abdul Hamid. Thank you so much in every point of this research for the precious time, advice, feedback, suggestions, and guidance. It was a great opportunity and pleasure to work and study under her guidance.

Besides, a special thank you goes to my beloved parents and siblings for their encouragement, support and prayers for the success of the project. I would also like to thank all my friends, especially my classmates and roommates for their infinite support.

Last but not least, my appreciation goes to those who have helped me directly and indirectly in completing this report. I am very thankful that lot of people have support and inspire me to carry out this project.

TABLE OF CONTENTS

CHAPTER 5: CONCLUSION AND RECOMMENDATION

REFERENCES

APPENDICES

LIST OF TABLES

LIST OF FIGURES

LIST OF ABBREVIATIONS

3D	-	Three dimensional
ABS	-	Acrylonitrile butadiene styrene
AM	-	Additive manufacturing
ASTM	-	American society for testing and materials
CAD	-	Computer-aided design
CAM	-	Computer-aided manufacturing
C-O	-	Carbon-Oxygen
FDM	-	Fused Deposition Modelling
FTIR	-	Fourier transform infrared
HIPS	-	High-intensity polystyrene
ISO	-	International Organization for Standardization
Mw	-	Molecular weight
N-H	-	Nitrogen-Hydrogen
PC	-	Polycarbonate
PDLA	-	Poly (D-lactic acid)
PDLLA	-	Amorphous poly (D, L-lactic acid)
PE	-	Percentage of error
PEEK	-	Polyether ether ketone
PEI	-	Polyetherimide
PET	-	Polyethylene terephthalate
PETG	-	Polyethylene terephthalate glycol
PLA	-	Polylactic acid
PLLA	-	Poly (L-lactic acid)
PPSF	-	Polyphenylsulfone
PSM	-	Projek Sarjana Muda
Pt	-	Platinum
ROP	-	Ring opening polymerization
RP	-	Rapid prototyping
SEM	-	Scanning electron microscope

SLA	-	Stereolithography
STL	-	Standard triangle language
Tg	-	Glass transition temperature
THF	-	Tetrahydrofuran
Tm	-	Melting temperature
TPU	-	Thermoplastic polyurethane
UFM	-	Universal tensile machine
UFS	-	Ultimate flexural strength
UTS	-	Ultimate tensile strength

LIST OF EQUATIONS

LIST OF SYMBOLS

%	-	Percent
°	-	Degree
°C	-	Degree Celsius
cm^{-1}	-	Centimetre power $^{-1}$
dl/g	-	Decilitre per gram
g/cm^3	-	Gram per centimetre cube
g/m^3	-	Gram per metre cube
g/ml	-	Gram per millilitre
g/mol	-	Gram per molecule
J/g	-	Joule per gram
K	-	Kelvin
Kg	-	Kilogram
kJ/mol	-	Kilo joule per molecule
kN	-	Kilonewton
lbs	-	Pounds
mg/l	-	Milligram per metre
mm	-	Millimetre
mm/min	-	Millimetre per minute
mm/s	-	Millimetre per second
N	-	Newton
N/mm^2	-	Newton per millimetre square
nm	-	Nano metre
$\Delta H°m$	-	Enthalpy
µm	-	Micron metre

CHAPTER 1
INTRODUCTION

This chapter describes the introduction of this research work, including the background, problem statement, objective, scope, and significance of the study. A study on the effect of humidity on the mechanical properties and microstructure of 3D printed PLA filament is carried out in this report.

1.1 Background

Additive Manufacturing (AM) or 3D printing is a modern manufacturing technology that has experienced massive growth over the last few years. 3D printing allows physical models and complex geometric structures to be produced with high precision and low cost. Due to the personalized and straightforward manufacturing of functional models, conceptual models, and prototypes, 3D printing has been hugely embraced by the military, automotive, medical, food industry, aircraft, and other allied industries (Mohamed, Masood & Bhowmik, 2015).

According to Zhang, Fan, and Liu (2020), Fused Deposition Modelling (FDM) is one of the mainly utilized AM processes because of its ease and availability of machinery with reasonable costs that employs thermoplastic materials as hot melt adhesive properties. Kwon *et al.* (2020) declared that FDM is among the most prevalent processes owing to its adaptability and low expense. Three-dimensional structures that integrate the primary material in layers via the heated nozzle of the FDM 3D printer are produced in the FDM process. The nozzle's horizontal and vertical directions are entirely funded by the software called computer-aided manufacturing (CAM).

Filaments from thermoplastics such as polycarbonate (PC), acrylonitrile butadiene styrene (ABS), and polylactic acid (PLA) are typically used as the raw material instead of metals in this technology because of their low melting point and its ability to melt continuously under heat and to be re-solidified after the heat is removed (Wang *et al.,* 2017). Consequently, this helps the FDM printer to produce a solid product after the semi-liquid extrusion of the raw material.

Different variables determine the properties of the filament's materials. Humidity is one of the key factors influencing the filament's properties, as shown in Figure 1. For example, if the polylactic acid (PLA) filament has been subjected to heavy moisture for an extended period, the filament has lost tensile strength at the time of printing which allows bubbles to emerge on the surface of the product (Valerga *et al.,* 2018). Additionally, PLA is susceptible to humidity, and changes in its properties are caused by exposure to high humidity. As humidity increases, it has been recorded that the elongation ratio, degradation rate, and average molecular weight decrease (Liu *et al.,* 2017).

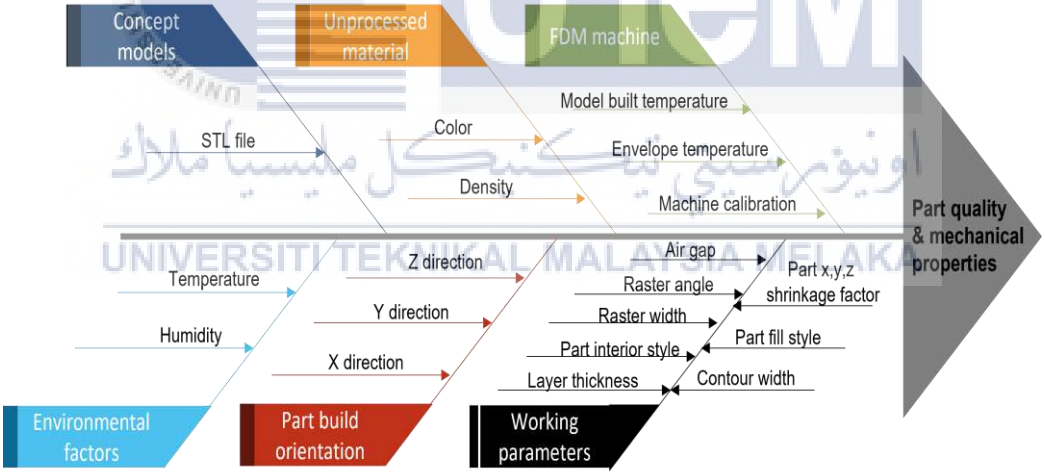

Figure 1.1: The cause-and-effect diagram of FDM process parameters (Mohamed, Masood & Bhowmik, 2015)

In this study, the effect of humidity on the mechanical properties, which includes tensile strength and flexural strength, and microstructure of the PLA printed parts exposed to various humidity environments was investigated.

1.2 Problem Statements

Polyesters are widely recognized for absorbing humidity, and the presence of moisture causes severe degradation events. The degradation is mainly caused by the hydrolysis of macromolecular chains, which significantly reduces molecular weight (Titone *et al.,* 2021). According to Mallick *et al.* (2018), polylactic acid (PLA) or polylactide is a biologically degradable and bioactive polyester consisting of building blocks of lactic acid. The filaments of PLA are made of fermented plant starch such as maize, sugarcane, sugar beet pulp, and cassava, making them distinct from other thermoplastics. Lesaffre *et al.* (2017) suggested that PLA is sensitive to such environmental restrictions. Exposure to different natural weather factors such as sunlight, rainfall, and humidity, typically contributes to the aging of the substance, which will affect both the physico-chemical and fire-resistant properties of the material.

Filaments made of PLA possess hygroscopic characteristics that appear to absorb moisture from the air, which contributes to inconsistent and poor printing quality (Dwamena, 2020). Suppose the filaments are stored in a humid environment. In that case, the water vapor tends to be absorbed, and steam is generated during the heating process, resulting in an imperfect product surface at the end of the process. In addition, this will lead to a generation of bubbles on the surface of the printed part. Valerga *et al.* (2018) stated that the filament had reduced tensile strength if the PLA filament is exposed to high humidity for an extended period. Therefore, the filaments must be kept sealed in a vacuum so that the filaments are still in a dry condition to ensure good printing quality. A study on the effect of humidity on the mechanical properties and microstructure of the 3D printed PLA specimens still lacks, which encouraged this study to be carried out. On the other hand, dehumidifying agents like silica gel or desiccant might be able to control the moisture content in the PLA filament. However, it is unknown to what extent it works and how it influences the PLA specimen's mechanical properties compared to the new PLA filament. Therefore, in this study, an attempt to investigate the influence of using these items on the mechanical properties of the PLA specimen is also conducted**.**

1.3 Objectives of Study

The objectives of this study are:

(a) To analyze the tensile strength of the 3D specimens fabricated using the non-exposed and moisture-exposed PLA filaments.

(b) To examine the flexural strength of the 3D parts produced from the non-exposed and moisture-exposed PLA filaments.

(c) To investigate the microstructure of the fractured 3D printed tensile samples using the Scanning Electron Microscope (SEM).

1.4 Scope of Study

The scope of this study are as follows:

(a) In this study, a 1.75 mm diameter of the PLA filament (light blue) was used for all conditions.

(b) The humidity level was decided through three conditions as follows:
   i. New PLA filament roll, which acts as the reference.
   ii. Used PLA filament roll stored in the vacuum bag, with the desiccant.
   iii. Used PLA filament roll stored in an open environment, exposed to a humidifier for variant of 24, 48, 72, 96, 120, and 150 hours.

(c) The printing parameters for all conditions were similar, with three replications of each conditional setting.

(d) The FDM machine, FlashForge's Adventurer3, was used to print the samples.

(e) The analysis of the tensile strength (ASTM D638 – Type IV) and flexural test (ASTM D790 of the FDM printed parts were carried out to investigate the influence of humidity on the quality of printing.

(f) The fractured tensile samples which have the closest maximum force value to the average value were used for the analysis of the microstructure using the scanning electron microscope (SEM) due to the limitation of laboratory usage during the Covid-19 pandemic outbreak.

(g) The samples used for SEM analysis were cut into 10 mm and then sputter-coated with 10nm thick of gold-palladium using SC 7620 Mini Sputter Coater machine.

1.5 Significance of Study

This study helps to analyse and examine the effect of moisture on PLA mechanical properties and microstructure. If the humidity is found to be affecting the quality and properties of the printed parts, a clear message to emphasize the importance of controlling this factor could be highlighted. Thus, it can improve the printing quality of parts produced from PLA and reduce the PLA waste. The reduction of 3D printing waste can promote sustainable 3D printing since the number of 3D printer users is increasing due to its affordability. In addition, the mechanical properties of the PLA filament, which is stored with desiccant in a vacuum bag, are found to be equivalent to the new PLA filament. This finding shows that the use of dehumidifying agents is sufficient to keep the humidity away from the used PLA filament to substitute drying rack, which is too costly for hobbyists. Therefore, it is hoped that this study could prove the effect of humidity on the printing quality of parts and simultaneously create awareness for all 3D printer users.

1.6 Organization of Report

In this study, there are five chapters consisting of introduction, literature review, methodology, result and discussion, conclusion and recommendation. Chapter 1 began with a study background, problem statement, objectives, and scope of the study. Chapter 2

comprised of previous study or research about the FDM process, PLA filaments, the influence of humidity towards the 3D printed parts, and the testing method of the mechanical properties. The methodology to achieve the stated objectives were explained in Chapter 3. Later, Chapter 4 analysed the tensile strength, flexural test and SEM analysis results. Lastly, the conclusion and recommendation about this study were discussed in Chapter 5.

CHAPTER 2
LITERATURE REVIEW

This chapter explains the content, steps, and every point that are related to the study. The data gathered from article, journal, published literature, books, magazine etc, which focuses on the 3D printing technology of FDM process. This chapter reviews PLA materials including its production and properties. Humidity and its influence towards 3D printing parts are also enclosed in this chapter. Besides, this chapter discusses the tensile strength, flexural test and SEM analysis.

2.1 Overview of 3D Printing

Charles (Chuck) Hull's SLA application, created in 1986, is the first AM technology that was introduced the last three years. Initially, this system was defined as rapid prototyping and production that involves the use of computerized 3D models to hold successive layers of materials on top of one another to develop a 3D shape. Automation and tool-free processes have reduced costs and time, allowed flexible production, realized design freedom and the number of higher parts possible (Tamez & Taha, 2021).

3D Printing is an enhanced technology because it can accommodate several materials that are not possible to produce extremely complex geometrical parts for various applications using traditional methods. Metals, alloys and their composites, ceramics, polymers, composites, biomaterials, and concrete are utilized in the construction of 3D components for medical, construction, engineering and education applications. There are also increasing benefits of material savings (Kumar & Sathiya, 2020).

Attaran (2017) declared several businesses have adopted AM technology and are continuing to benefit from investment in real industry over the last few years. Technology is ripening and has made its way into a variety of industries. It is also used in prototyping and distributed development, allowing AM to be embraced by the next generation of consumers. Technology is slowly evolving as a valuable way to increase internal efficiency. It is one of the most interesting and hottest trends today in architecture and marketing.

2.2 Fused Deposition Modelling (FDM)

Fused Deposition Modelling (FDM) is a 3D printing technology that shapes thermoplastic-based substance extrusion structures supplied in filament form. After the loaded machine details, material in the form of liquid is deposited layer by layer on the building table. FDM technologies belong to the community of 3D printers focused on extrusion (Haryńska *et al.,* 2020).

For modelling, prototyping, and manufacturing applications, FDM is now frequently used. Based on Figure 2.1, the material is melted into a liquid state in a liquefier head and then selectively deposited by a nozzle tracing the cross-sectional geometry of the components to create 3D structures in a layer by layer directly from a CAD model (Mohamed, Masood & Bhowmik, 2015).

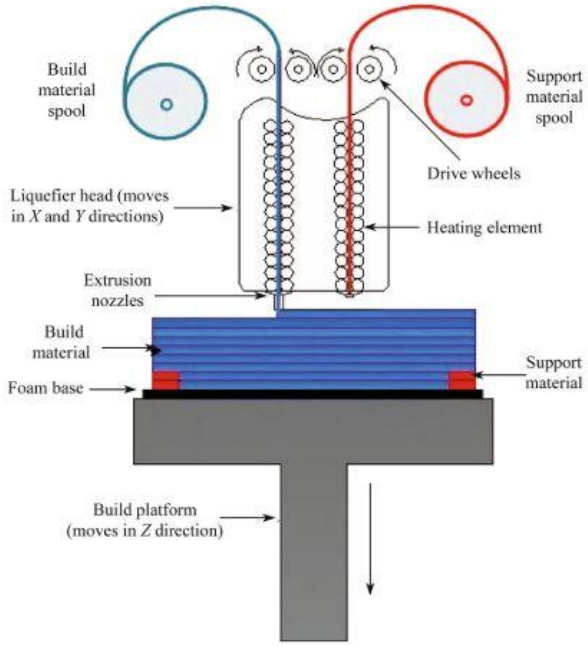

Figure 2.1: Process parameters of FDM (Mohamed, Masood & Bhowmik, 2015)

2.2.1 Process parameters

Today, the additive production processes like FDM are needed to provide superior component efficiency, high efficiency, protection, low production cost, and shorter time. The additive production process conditions for each design must be calculated to satisfy consumer requirements and satisfaction. The main performance of the additive production process relies on the appropriate set of process parameters (Mohamed, Masood & Bhowmik, 2015).

It is important to set optimal process conditions as it leads to higher consistency of product, increased efficiency, improvement in the dimensional accuracy, elimination of unacceptable waste, and significant amounts of scraps. It also reduces the time and costs of the production. Due to various contradiction parameters that affect the consistency and material properties of the component, FDM is a complex process that poses great difficulties in deciding optimum parameter. Masood (1996) stated that the quality of the part and mechanical properties of the parts produced can be calculated by the correct selection of process parameters.

2.2.2 Materials

Many typical additives are used in the additive production (plastic, metal, sand, wax, gyps, etc.). A printable content must be chosen, which is a tough choice to take in the overwhelming probability when printing a sample. Researchers are beginning to focus more on the adverse effects of pollution and waste. Thus, the concept of "eco-friendly" biodegradable, recyclable and compostable materials was developed.

After all, regardless of its low prices, non-biodegradable materials dominate the rapid prototyping materials market. The materials are typically rated in three ways which are consistency, mechanical efficiency, and process but the following graph illustrates the main decision requirements for the choice of print material (visual quality, easy printing, impact resistance, maximum tension, layer adhesion (isotropy), heat resistance, and split elongation) (Mazurchevici, Nedelcu & Popa, 2020). The findings of studies on the material properties of major pure polymers used in the FDM technology over the past years are briefly described in Figure 2.2.

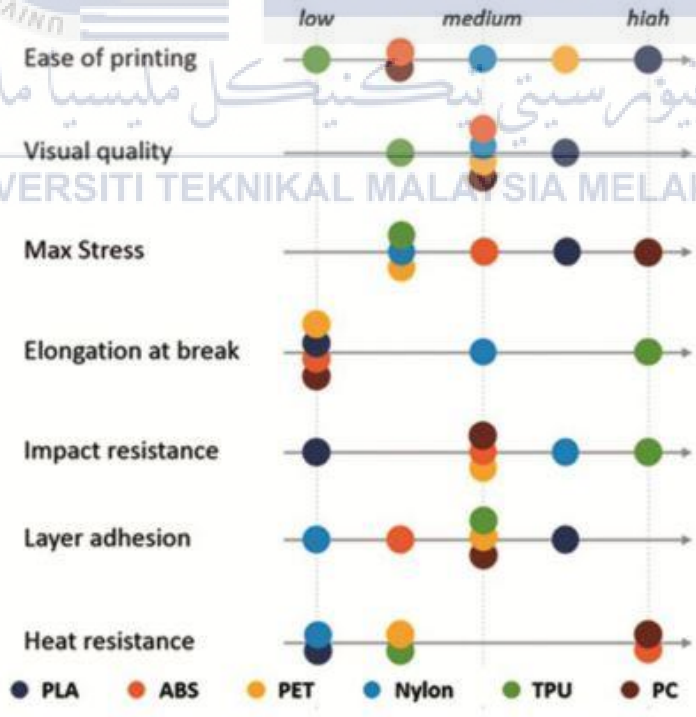

Figure 2.2: Comparison of thermoplastic materials (Mazurchevici, Nedelcu & Popa, 2020)

Dey and Yodo (2019) described the usually used filament materials as below:

a. ABS: Amongst the most popular materials applied to manufacture parts through FDM, a thermoplastic and amorphous polymer. It is a copolymer manufactured from acrylonitrile, butadiene, and styrene; ABS has two significant mechanical properties of impact resistance and hardness. ABS is not organically degradable but poses a decreased chance of jamming a dust.
b. PLA: A biodegradable thermoplastic, which is frequently used in FDM. In order to process prototypes and working sections of high quality, it takes less energy and temperature. A variety of 3D desktop printers use PLA as a filament, because there is no heated bed required, though a printing nozzle is liable to be jammed. PLA is tougher than ABS, has a low tensile strength, warp, and low ductility. PLA designed components required extra care compared with ABS for the post-processing.
c. PC: A category of thermoplastics recognized for their, resilience, strength, and hardness, with some being translucent. They are a commodity that is known for their high resistance. They are heat tolerant high-temperature thermoplastics, excellent layer for layer binding, and have a good surface consistency.
d. PEEK: A thermoplastic with excellent heat tolerance, chemical consistency, and mechanical properties. In contrast to PLA and ABS, it has higher mechanical properties.
e. PEI: Commonly used in the transport sector because of its high strength to weight ratio of low smoke production and small toxicity of smoke. During printing, it needs an excessive bed and extrusion temperature.
f. Nylon: The filament used to print parts with high flexibility and more durability. It is incredibly durable and resistant to impact, but it is heavily moisturized. Nylon is as much warp as ABS. Nylon retains atmospheric moisture when it is hygroscopic, just as many other filaments are seen in FDM. Moisture accumulation deteriorates the features of the filaments and induces partial deterioration.
g. Other materials: Materials such as high-intensity polystyrene (HIPS, PPSF), refined polyethylene teriphenyl glycol (PETG) or thermoplastic (TPU), bio-composite filaments, ceramic filaments, and other composite materials are rarely used as filament materials. Any of these materials continue to be created or are not widely available on the market.

2.3 Polylactic Acid (PLA)

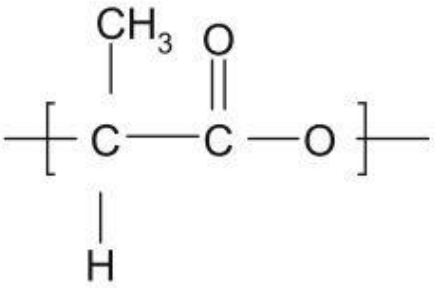

Poly(lactic acid)

Figure 2.3: PLA structure

Bio-based polymers are plastics from biological sources like starch, cellulose fatty acids, carbohydrates, proteins, and other sources consumable by microorganisms. Thus, PLA is a biodegraded material as it is formed by renewable sources such as beets and maize shown in Figure 2.4.

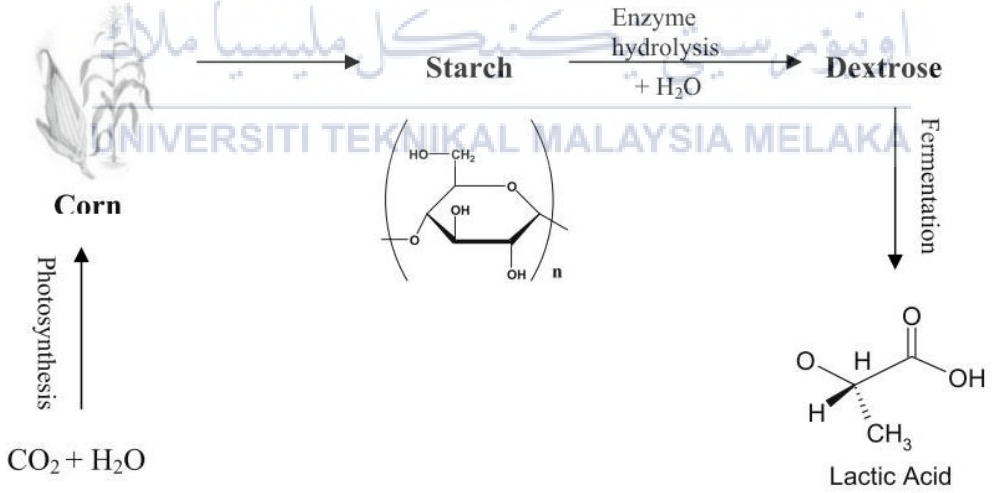

Figure 2.4: Production of lactic acid from renewable source (Avinc & Khoddami, 2009)

PLA is produced into an overall petrochemical derivative component using lactides. This material can be produced in big quantities by agricultural product fermentation process. There are several various methods, including extrusion and injection moulding, used for manufacturing PLA (Raza & Singh, 2020).

2.3.1 Production of PLA

Gupta, Revagade, and Hilborn (2007) stated PLA processing includes lactic acid monomer synthesis and polymerization. HOCH3CHCOOH lactic acid is a basic chiral molecule that occurs as two enantiomers, L- and D-lactic acid shown in Figure 2.5, where the polarized light plane rotation of L isomer is clockwise while the D isomer rotates in counterclockwise direction.

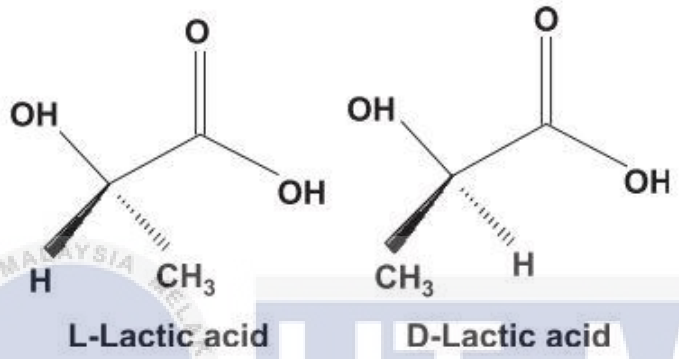

Figure 2.5: Optical isomers of lactic acid

Two ways of lactic acid polymerization to high molecular weight PLA are; (a) direct lactic acid polycondensation (LA); (b) polymerization of ring-opening (ROP) through the cyclic dimer (lactide) (Gupta, Revagade, & Hilborn, 2007) (Murariu & Dubois, 2016). Besides, Lim, Auras, and Rubino (2008) expressed that condensation of azeotropic dehydration can also be used to produce PLA as illustrated in Figure 2.6.

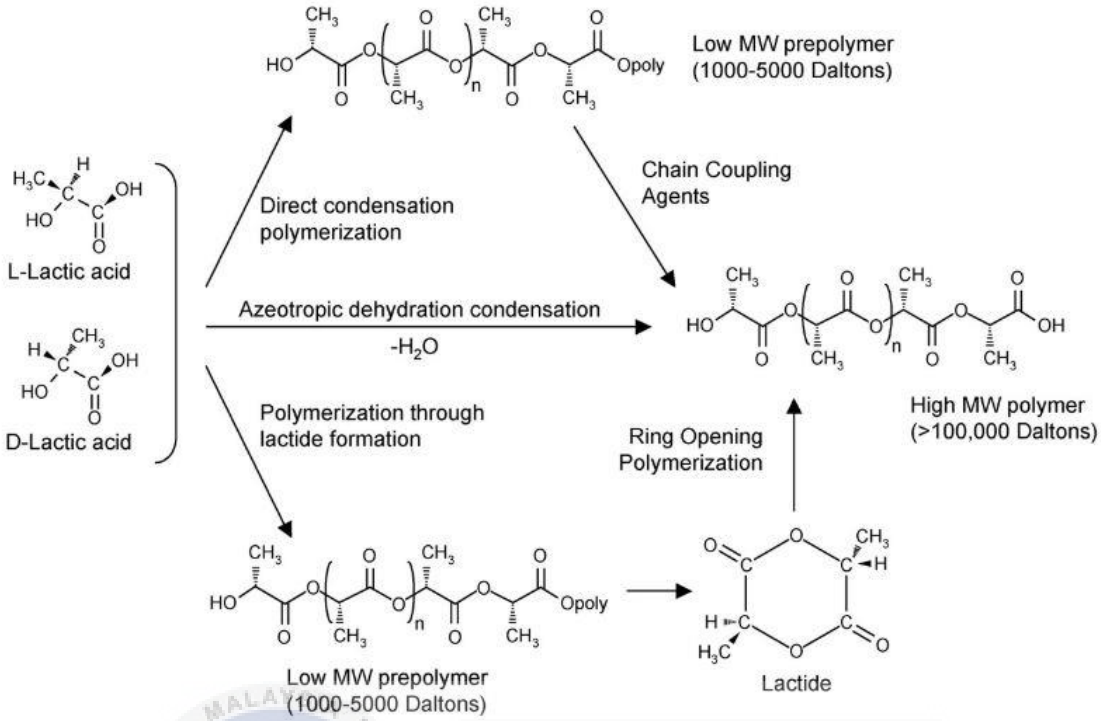

Figure 2.6: Polymerization steps of PLA (Lim, Auras & Rubino, 2008)

According to Avinc and Khoddami (2016), the direct lactic acid polycondensation is achieved at high vacuum and high temperatures. The water produced by the condensation reaction will be extracted using solvent. This road was used to manufacture PLA polymers by Carothers. Due to problems of extracting water and impurities, the substance obtained appears to have low or moderate molecular weight (Mw 10,000-20,000).

In fact, lactide is a cyclic dimer produced under mild conditions and without solvent, by removing water. The high molecular PLA is usually obtained by polymerization of ring-opening (ROP) through the cyclic dimer (lactide) using a stannous catalyst on the ground of octoates, although other catalysts and polymerization methods are also used for laboratory demonstrations. Furthermore, biosynthesis of PLA using enzymes is a new task for both science and industry (Murariu & Dubois, 2016).

It is more feasible to manufacture high molecular weight PLA polymers by direct polycondensation in an azeotropic solution and even to add certain catalysts. By adding molecular sieves, the azeotropic solution helps to reduce the distillation pressures and enables PLA separation from the solvent. The range and content of catalysts, the percentage of solvent volume, and the reaction time for PLA preparation have been studied. The findings

found to achieve a molecular weight of PLA of 6.6×10^4 g/mol, using better laboratory tools, the correct complex catalyst, and solvent volume ratio (Jamshidian *et al.,* 2010).

2.3.2 Properties of PLA

PLA has many properties like many other synthetic fibres since it is a melt-processable fibre from a vegetable source (Dugan, 2001).

White powder of lactic acid homopolymer occurs at room temperature with Tg = 55°C and Tm = 175°C. PLA is a colourless, glossy, solid thermoplastic composite with high molecular weight with properties identical to polystyrene. Four distinct materials can be formed by L- and D-lactic acid: poly(D-lactic acid) (PDLA), a normal chain structure of crystalline material; poly(L-lactic acid) (PLLA), a regular chain structure of hemi crystalline; amorphous poly(D,L-lactic acid) (PDLLA); and meso-PLA, acquired by polymerization of meso-lactide (Xiao *et al.,* 2012). The several physical and chemical properties of the PLA are displayed in Table 2.1.

Table 2.1: Physical and chemical properties of PLA (Xiao *et al.,* 2012)

Properties	PDLA	PLLA	PDLLA
Solubility	All are soluble in benzene, chloroform, acetonitrile, tetrahydrofuran (THF), dioxane etc., but insoluble in ethanol, methanol, and aliphatic hydrocarbons		
Crystalline structure	Crystalline	Hemicrystalline	Amorphous
Melting temperature (T_m)/ °C	~180	~180	Variable
Glass transition temperature (T_g)/ °C	50-60	55-60	Variable
Decomposition temperature/°C	~200	~200	185-200
Elongation at break/ (%)	20-30	20-30	Variable
Breaking strength/ (g/d)	4.0-5.0	5.0-6.0	Variable
Half-life in 37°C normal saline	4-6 months	4-6 months	2-3 months

Based on the table 2.1, PDLA, PLLA and PDLLA are soluble in benzene, chloroform, acetonitrile, THF, dioxane, etc. However, they happened to be insoluble in ethanol, methanol, and aliphatic hydrocarbons. Depending on the article size and form, ratio of isomer and

temperature, PLA has a degradation half-life in the atmosphere ranging from 6 months to 2 years.

The melting temperature (Tm) and glass transition temperature (Tg) of PLA decrease with lower levels of PLLA. The physical properties of the PLA are based on its Tg, including density, heat, and mechanical and rheological characteristics. PLA appears to be crystalline with a PLLA value greater than 90 percent, while the lower optically pure tends to be amorphous (Henton *et al.,* 2005).

Tg and Tm are essential physical parameters for to predict to its behaviour of semicrystalline PLA. The melt enthalpy measured for 100 percent of crystallinity ($\Delta H°_m$) of enantiopure PLA is 93 J/g. The Tm and crystallinity amount depends on the polymer molar mass, thermal background, and purity. The density was stated as 1.248 g/ml and 1.290 g/ml respectively for amorphous and crystalline PLLA. Strong PLA density has been stated as 1.36 g/cm3 for L-lactide, 1.33 g/cm3 for meso-lactide, 1.36 g/cm3 for crystalline, and 1.25 g/cm3 for amorphous PLA, respectively (Farah, Anderson & Langer, 2016).

After several months of exposure to moisture, PLA degrades mainly by hydrolysis by two steps. Firstly, the spontaneous non-enzymatic chain breaking of the groups of esters leads to a decrease in molecular weight. Secondly, before the lactic acid and low molecular weight oligomers are spontaneously metabolized by microorganisms to create carbon dioxide and water, the molecular weight is decreased. The degradation rate of the polymer is determined primarily by the polymer. The polymer degradation rate would be influenced by any factor influencing reactivity and accessibility, such as particle size and form, temperature, moisture, crystallinity, percent isomer, residual lactic acid concentration, molecular weight, water diffusion, and metal impurities from the catalyst (Lasprilla *et al.,* 2012).

Some of physical characteristic of PLA studied by Gupta, Revagade and Hilborn (2007) are listed in Table 2.2.

Table 2.2: Physical properties of PLA (Gupta, Revagade & Hilborn, 2007)

Property	Units	Condition	Value
Degree of crystallinity X_c	%	L-PLA	0–37
Density ρ	g/cm^3	Amorphous	1.248
		Single crystal	1.290
Heat of fusion ΔH_f	KJ/mol	L-PLA complete crystalline	146
		L-PLA fiber	
		As-extruded	2.5
		After hot drawing	6.4
Heat capacity C_p	J/K/g	L-PLA with	
		$Mv = 5300$	0.60
		$Mv = (0.2–6.91) \times 10^5$	0.54
Glass transition temperature	K		326–337
Melting point	K		418–459
Decomposition temperature	K		500–528
Swelling in water %		pH 7 buffer	2
Intrinsic viscosity (η) in chloroform at 25 °C	dl/g		3.8–8.2
Radiation resistance	G value	Under nitrogen	
Co^{60} in benzene solution, 30 °C		Chain scission	26.5
		Cross linking	4.5
In water		Chain scission	
		Cross linking	23.0
			6.5
IR peaks	cm^{-1}		
OH (alcohol/carboxylic)			3700–3450
–C = O			1750–1735
–COO			1600–1580
C-O			1200–1000
CH			950–700

PLA has elevated hydrophilicity. It has a higher natural hydrophilicity than most other thermoplastic polymers, including polypropylene, nylon, and PET, since water molecules have access to the polar oxygen linkages in the PLA molecule. This increase both the wettability of the fibre and the transfer of moisture vapor. PLA fibers are not as humid as cotton, but when they replace fibers such as PET or nylon, they may offer increases in moisture transport (Karthik, 2004).

PLA shows greater alkali exposure than PET. Due to this sensitivity, any loss of fibre intensity during subsequent wet processing is found if caution is not taken in dyeing and finishing the fibre. PLA has a surface cohesion that gives a scroop-like property to the polymers. When the materials are brushed against each other, the scroop of polymers causes a vibration or 'crunchiness' to be felt, most likely caused by a stick-slip movement as they slide past each other. This function of PLA fabrics can affect durability and thus cause problems by resisting recovery after deformation in some applications (Avinc & Khoddami, 2016).

2.4 Humidity

Humidity or moisture is the volume of vapor which can be found in gas sample, and it is classified into two categories:

- Absolute humidity: Water vapor mass available per unit of gas volume (mg/litre or g/m3).
- Relative humidity: Water vapor ratio available in the gas to the maximum water vapor that the gas can produce might be the ratio of the water vapor occur in the gas (percent). Relative humidity is used most widely and is measured more easily.

If the temperature increases, the amount of water vapor a given volume of air can contain will rise leads to a change of relative humidity temperature. The air is completely saturated with water vapor at 100 percent of relative humidity. The overall volume of water vapour produced also reduced when gas temperature decreases which will increase the relative humidity higher than 100 percent and condensation can happen.

2.4.1 Measurement of relative humidity

There are several methods can be used to measure humidity as stated by Lewis and Chambers (2020).

2.4.1.1 Wet and dry bulb hygrometer

The hygrometer comprises two thermometers, a dry bulb and a wet bulb. Their titles suggest that the dry bulb is dry in the air and the et bulb is surrounded by a wick of cotton dip in the water. In humidity calculation the wet bulb plays the primary function. The rate of evaporation varies based on the humidity of the atmosphere: the lower the humidity, the greater evaporation, and the lower it is. The psychometric scale is used to measure the relative humidity from the temperature differential of the two thermometers. The differential temperature between two glass thermometers is utilized to measure the relative atmospheric humidity due to the residual vaporization heat.

Figure 2.7: Wet and dry bulb hygrometer (Source: IndiaMART)

2.4.1.2 Hair hygrometer

This approach requires a fibre strand under tension and connected to a pointer. When water is consumed, the strand grows in length resulting the pointer going around a standard. Based on the atmospheric humidity, the amount of water consumed by the strand is. Traditionally, this process used hair of human but modern hair hygrometers use cellulose strands or nylon. The reaction time of this approach is slow and as opposed to other approaches it is less precise. However, the hair hygrometer is widely used in theatre setting due to its versatility and cheap price.

Figure 2.8: Hair hygrometer (Source: IndiaMART)

2.4.1.3 Regnault's hygrometer

A dew point hygrometer that typically consists of a thermometer and high thermal conductivity silver tube containing ether. The fluid is bubbling in and out of the ether so that it evaporates. The tube point at where condensation is detected on the outside of the tube is reported. The relative wetness at the point of dew is 100% and at all temperatures the relative humidity is then determined by a saturated steam pressure table. The accuracy of digital instruments is better as electronic sensors are used to sense immediately dew dots and a cooled mirror instead of the ether-filled glass tube.

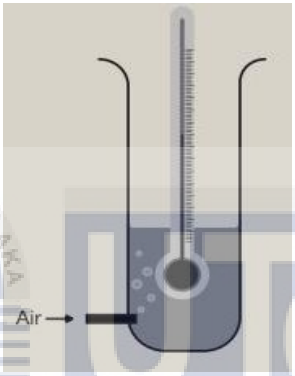

Figure 2.9: Regnault's hygrometer (Lewis & Chambers, 2020)

2.4.1.4 Electronic hygrometer

Electronic hygrometers have either a capacitor or a resister. Water vapor exposure increases the resistance or capacitance - relative humidity is quickly determined from this shift. Electronic hygrometers are compact and measure alterations in atmospheric humidity easily.

Figure 2.10: Electronic hygrometer (Source: extech.com)

2.4.2 Measurement of absolute humidity

2.4.2.1 Mass spectrometry

Mass spectrometry may be used to measure the water vapour found in air sample in a highly precise manner. The ionization of molecules by electrons happened inside the sample and are diverted onto a sensor by a magnetic field. The ratio of mass charge of the particles influences the sum of deflection is dependent on. The amount of all type of molecule is determined until isolated and estimation of humidity occur. For most clinical uses, the equipment is heavy and thus is not practical, but can be used to calibrate other procedures.

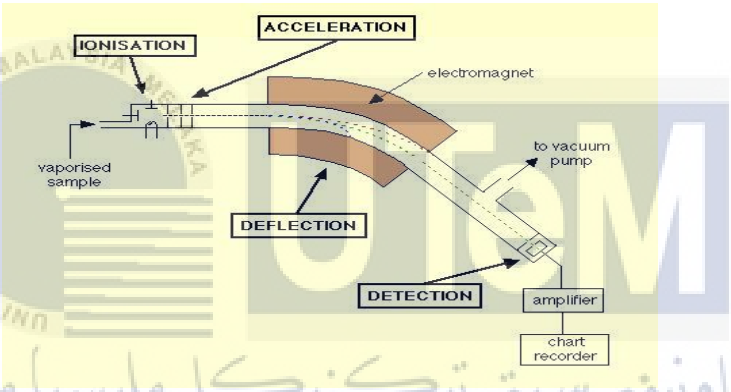

Figure 2.11: Mass spectrometry (Source: chemguide.co)

2.5 Humidity Effects on 3D Printing

The PLA filament will swell up to 40 micrometres before reaching its saturation point after 150 hours (6 days) under normal conditions. Tight tolerances and incredibly limited layer heights rely on 3D printers. Before the print even starts, an expanded filament diameter of 20 to 40 microns (about the width of a human hair) will destroy a build even before it starts (What Effect Does Moisture Have on 3D Printer Filament Storage?, 2020).

There are possible moisture content signs for a failed 3D printing build such as:

a. The filament breaks or creates noise to pop when the filament is forced into the extruded filament.

b. Holes at the end of modules
c. Extruder tip bubbles with short, stringy or drooly steam bursts
d. The filament is not going to stick to the printing bed.
e. Repeated compilations tend to be contradictory or refuse to modify variables.
f. The extrusion engine stops, but the filament keeps coming out.
g. The extruder engine begins, but filament extrusion is deferred.
h. Parts become fuzzy, delicate, and easily crack.
i. Jams from the extruder

Kakanuru and Pochiraju (2020) tested the microstructure and the mechanical efficiency of ULTEM 9085 3D printed components for the effects of moisturized filament. They observed that with an increase of moisture in the filament, the tensile strength and failure strain of the printed parts decreased considerably. In addition, Kariz, Sernek, and Kuzman (2018) investigated the effect of moisture on 3D printed samples made from wood-PLA filaments, claiming that as the content of wood increased in all climates, the moisture content of the specimens increased, causing mechanical and bending properties to decrease.

Chola (2017) found that the mass flow rate is directly related to the moisture content of the PLA filament. The filament with the least viscosity and the fastest mass flow is the one with the most moisture. He then concluded that PLA filaments must be stored under strict conditions. Moreover, Kwon *et al.* (2020) claimed 3D objects printed using PLA filaments that are exposed to higher humidity are easy to fracture and become less uniform. However, the tensile strength of a 3D printed object is increased, difficult to break and is more uniform when PLA filament is subjected to low moisture.

Besides, a study by Titone *et al.* (2021) showed that absorption of moisture through filament results in a reduction in elastic modulus and stress, as well as an increase in elongation at break. These alterations have been linked to a potential hydrolytic deterioration, namely the plasticizing effect of the moisture absorbed by the specimens. Similarly, Yu (2012) confirmed that the absorbed moisture substantially plasticized urethane foams because water molecules can serve as a plasticizer, lowering the Tg while also increasing the fracture strain.

2.6 Tensile Test

Tensile testing is important in order to understand the characteristics and behaviour of various materials under the tensile load. Consequently, the test is conducted by engineers to gain valuable knowledge regarding the properties of a specimens. It measures the force necessary to break a plastic or composite specimen, and the degree where the specimen expands or elongates to the breaking point. Singh *et al.* (2020) stated the maximum value of strain is reached at the smallest cross section in the neck region in tensile testing.

Saba (2018) expressed tensile testing complies with standards such as ASTM D 638, ASTM C 297, ASTM D 3039, ISO 527-5 and ISO 527-4. Durga Prasada Rao *et al.* (2019) tested the tensile strength of carbon fibre PLA specimens formed by FDM using the universal testing machine (UTM) following the ASTM D638 standard. In addition, Yadav *et al.* (2020) also used the universal testing machine with speed of 5mm/min with ASTM D638 standard to evaluate mechanical strength of 3D printed PLA parts by free form fabrication. Figure 2.13 illustrates the tensile test setup.

Figure 2.12: Tensile test setup (Yadav *et al.,* 2020)

In 2020, Kwon *et al.* measured the tensile strength of 3D printed PLA specimens by comparing the results obtained through tensile testing using the stress-strain curves. The

relationship between stress and strain is represented by stress-strain curves, and each material has its own stress-strain curve, independent of volume or size. If a material, such as PLA, is subjected to humidity and the stress-strain curve changes, the PLA characteristics have altered as a result of the humidity. Kwon *et al.* (2020) also concludes in their study; the tensile strength is increased (difficult to break and more uniform) when PLA filaments is exposed to low humidity level.

2.7 Flexural Test

A flexural test is commonly used to determine flexural strength and modulus. The greatest stress at the outermost fibre on either the compression or tension side of the specimen is termed as flexural strength. The slope of the stress vs. strain deflection curve is used to compute flexural modulus. Both values of flexural strength and flexural modulus are used to measure the ability of the sample to sustain flexure or bending forces.

Kumar *et al.* (2020) tested the flexural strength of 3D printed prototypes of thermoplastic matrix reinforced with multi-materials using universal tensile testing machine (UTM) following ASTM D790 standard. Dhinesh *et al.* (2020) and Raj *et al.* (2018) also used ASTM D790 with lengths of 127mm, widths of 12.7mm, and depths of 3.2mm for flexural testing in their study. Pugalendhi *et al.* (2019) performed the flexural testing on the 3D printed specimens by using Zwick universal testing machine with capacity ranges of 0–100kN and speed of 50mm/min. Figure 2.14 illustrates the flexural test setup.

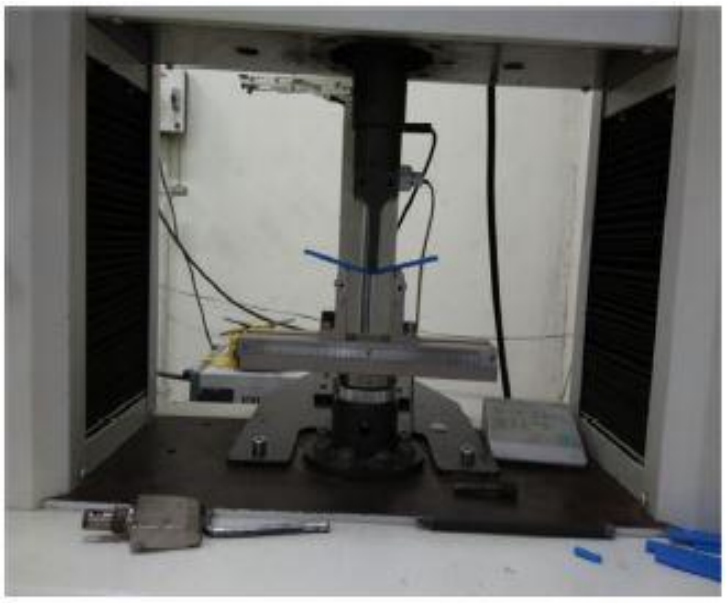

Figure 2.13: Flexural test setup (Raj et *al.,* 2018)

2.8 Scanning Electron Microscopy

Scanning Electron Microscope (SEM) is a technique used to analyse a microstructure of a sample surface using an electron focus beam to generate a high-resolution picture. As claimed by Goldstein (2012), SEM is the most widely utilised microstructure scanning. SEM provides an image that depicts the surface composition and typography of a substance. This approach of scanning a fracture component is used in analysing the mechanical characteristics of 3D printed objects. The surface images were taken using a Carl Zeiss Evo 50 at 10.00kV accelerating voltage for 25x and 50x magnification power at secondary electron according to a recent study by Hamid *et al.* (2019).

Kakanuru and Pochiraju (2020) have found large voids in the SEM image of sample which result from the disintegration of the material. Figure 2.15 clearly shows the difference in geometry of voids between aged and unaged specimens.

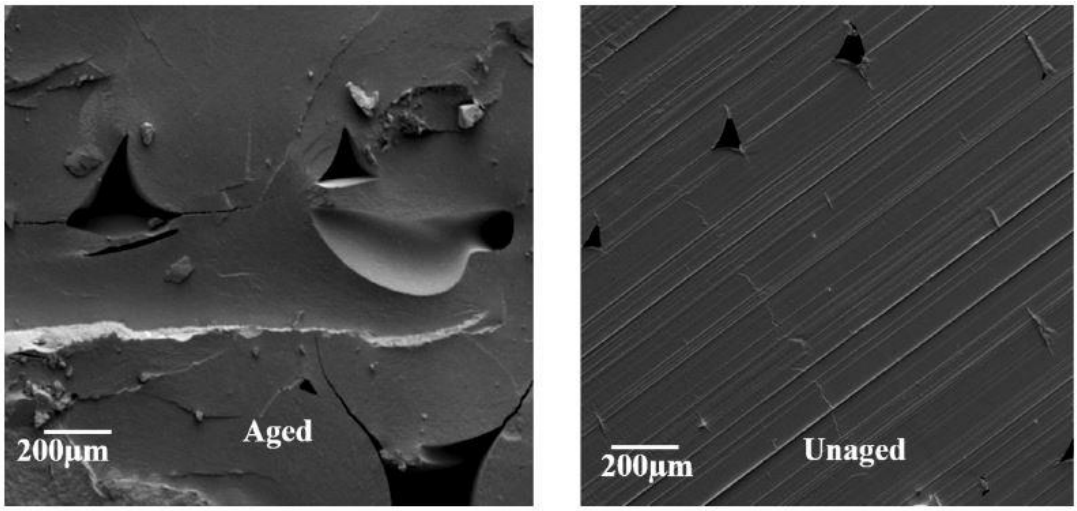

Figure 2.14: The microstructure of 3D printed PLA (Kakanuru & Pochiraju, 2020)

Zaldivar *et al.* (2018) studied the effect of initial filament moisture content on the microstructure and mechanical performance of ULTEM®9085 3D printed parts. Figure 2.16 illustrates the fracture surfaces of dog bones produced using ULTEM®9085 filaments with differing moisture content (control, 0.1, 0.16, 0.4, 0.8%).

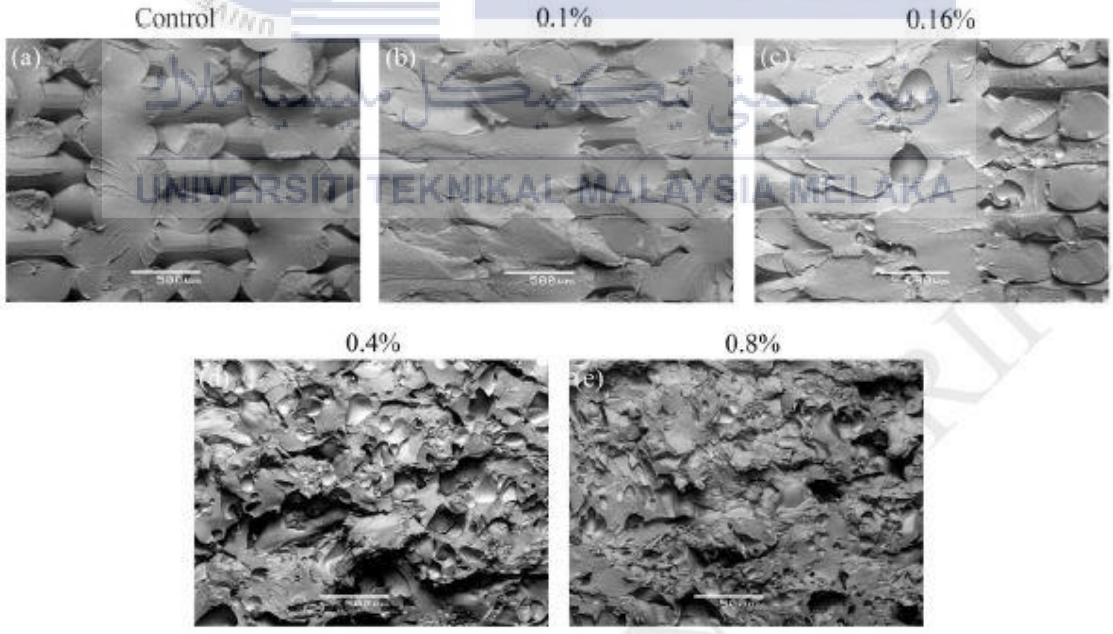

Figure 2.15: Fracture surfaces of dog bones produced using ULTEM®9085 filaments (Zaldivar *et al.,* 2018)

2.9 Sputter-coating

Sputter-coating is a technique for applying a functionally thin layer on a surface. Scanning electron microscope (SEM) may be used to examine the nanostructure characteristics of materials in a variety of applications. Some samples may be more difficult to scan than others. To put it another way, the procedure must go through the sputter-coating process in order to acquire a high quality image. Sputter-coatings can be made of both conductive and non-conductive materials. Sputter-coating is usually done in a vacuum chamber filled with either a chemically inert gas or a reactive gas, with a substrate positioned to face the coating material's target. According to Jo *et al.* (2018), 8-nm thick Platinum (Pt) coating is used to coat the fracture component in order to ensure a clear scanning image throughout the SEM procedure.

2.10 Summary

All in all, there is still a gap in analysing the effect of humidity towards mechanical properties and microstructure of PLA specimens. However, some details are followed as a guide from the literature. To begin, the PLA filaments were set to be subjected to humidity (humidifier) for 150 hours, or about 6 days. The tensile testing referred the ASTM D638 standard using universal testing machine with speed of 5mm/min. Next, the flexural testing followed ASTM D790 standard with speed of 50mm/min. Besides, the fractured samples were sputter-coated before SEM analysis. Lastly, this study examined the findings and equate them with the previous studies.

CHAPTER 3
METHODOLOGY

This chapter discusses the adopted procedures for the completion of this study. A detailed explanation of the selected mode of analysis used and the data collection method is elaborated. The research plan is designed to achieve the stated objectives in Chapter 1 to study the effect of humidity on mechanical properties and microstructure of 3D printed PLA filament.

3.1 Process Flow of the Study

The study consists of two parts, PSM 1 and PSM 2. It relies on three sections for PSM 1: an introduction, analysis of literature, and methods used to accomplish goals. PSM 2 is more on implementing the research plan in PSM 1, which contains the 3D printing procedure, result and discussion, and conclusion, including the recommendation for any improvements.

This study used both qualitative and quantitative methods. The secondary method is applied for the qualitative by reviewing books, journals, and articles related to the study. On the other hand, the primary method is used for the quantitative, involving experimental and observation approaches. The study flow continues from the selection of the title to the end of the research according to the flow chart as shown in Figure 3.1.

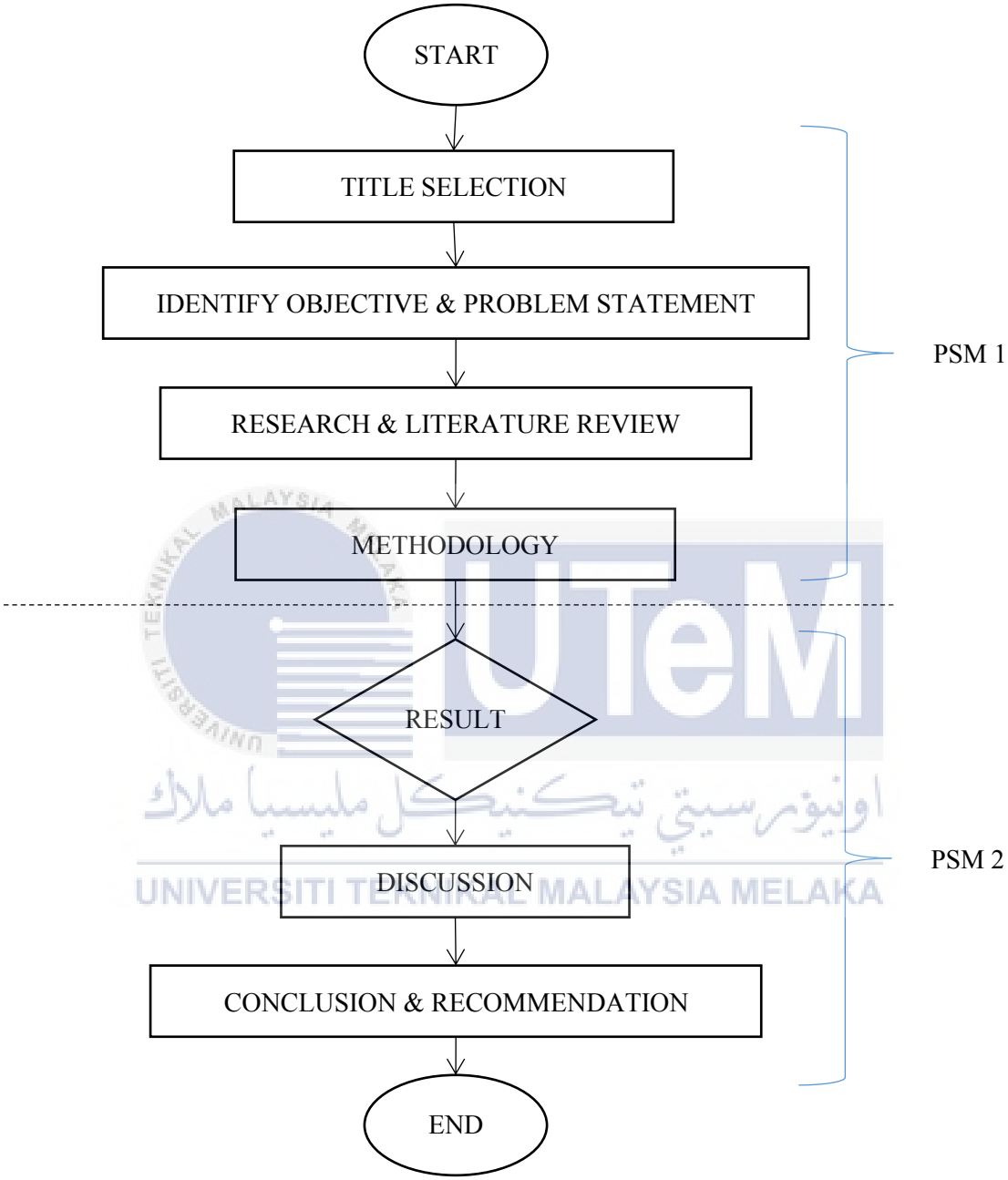

Figure 3.1: Process flow of PSM 1 and PSM 2

3.2 Relationship between the Objectives and Methodology

Table 3.1 demonstrates the implications of the method used to achieve the goals of the study. The suitable approaches for each objective have been used to satisfy possible quality requirements to accomplish this study.

Table 3.1: Implications of methodology used in the study

Objective	Method
(a) To analyse the tensile strength of the 3D specimens fabricated using the non-exposed and moisture-exposed PLA filaments.	FDM Process: • Machine: FlashForge's Adventurer3 • Material: PLA filaments • Filament Color: Light Blue Tensile Test: • Shimadzu AGS-X universal testing machine
(b) To examine the flexural strength of the 3D parts produced from the non-exposed and moisture-exposed PLA filaments.	Flexural Test: • Shimadzu AGS-X universal testing machine
(c) To investigate the microstructure of the fractured 3D printed tensile samples using the SEM.	Sputter-coating: • SC7620 Mini Sputter Coater machine SEM Analysis: • Scanning electron microscope (SEM) machine

3.3 Flow Chart of Methodology

The flow chart is used to explain the research plan of the study in achieving the stated objectives. Figure 3.2 shows the flow chart of this study.

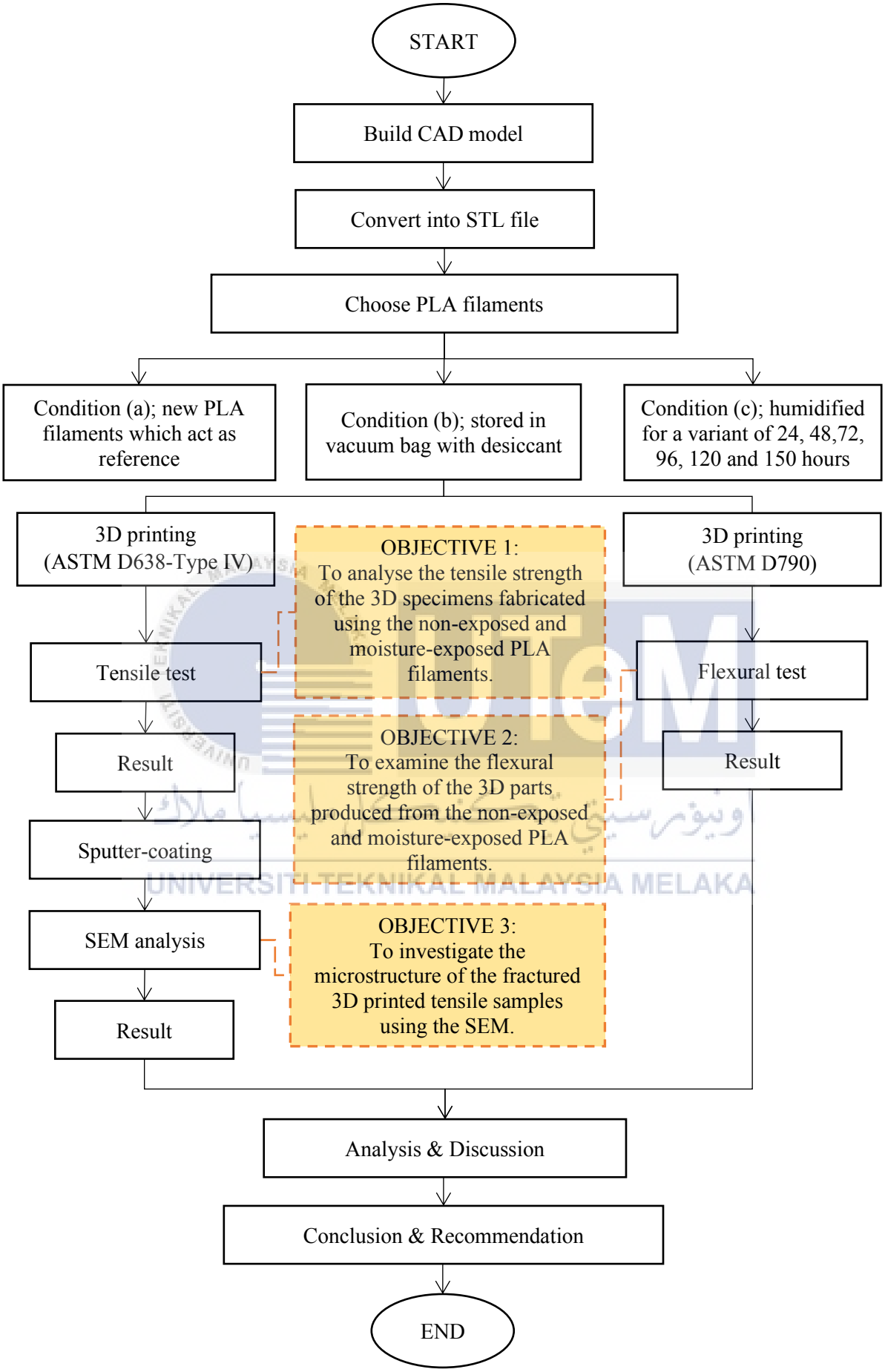

Figure 3.2: Flow chart of methodology used to achieve stated objectives

3.4 Preparation of PLA Filaments

The material used in this study is PLA, as shown in Figure 3.3. There are two types of storage used to store the PLA filaments; (a) open environment with exposure to a humidifier for a variant of 24, 48, 72, 96, 120, and 150 hours; (b) vacuum bag, with the desiccant where it acts as a dehumidifying agent to maintain the dryness of the PLA filaments. The specification of the PLA filaments is stated as below:

- Filament Color: Light Blue
- Filament diameter: 1.75mm
- Length: 325 meters
- 1kg (2.2 lbs) of filament
- Printing temperature: 190°C to 220°C
- Manufacturer: Cixi Lanbo Printer Consumable CO., LTD.

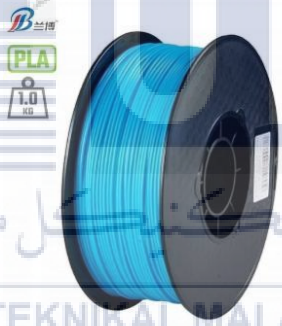

Figure 3.3: PLA filament

In this study, the humidity level was decided through three conditions as follows: (a) new PLA filament roll, which acts as the reference; (b) Used PLA filament roll stored in the vacuum bag, with the addition of desiccant; (c) Used PLA filament roll stored in an open environment, exposed to a humidifier for a variant of 24, 48, 72, 96, 120, and 150 hours. A humidifier is recognized as equipment used to enhance the humidity (moisture) level in one room or a whole building. Humidifiers are usually used to increase moisture content in the air, usually during the winter which the air is dry. Thus, the purpose of using a humidifier in this study was to expose the PLA filaments to moisture before 3D printing to investigate if the existence of water influences the mechanical and microstructure of the 3D printed items.

3.5 CAD Model

An integral part of 3D printing is CAD. A 3D printer will not have the instructions it requires to create a sample or device without a CAD register. The CAD model specifies the 3D printer's amount of material it requires to deposit and where to deposit the material. In this study, a CAD model is set to perform the 3D printing process. Based on the ASTM-D638 (Type IV) standard, 3D specimens with dimensions in mm, as shown in Figure 3.4, are used. Type IV is chosen due to the limitation of the build-up size of the selected 3D printer used in this study. Besides, 3D specimens following ASTM D790 with dimensions in mm illustrated in Figure 3.5 are used for flexural testing. The CAD model for both 3D specimens in Figure 3.6 and Figure 3.7 is drawn using CATIA V5R19 software.

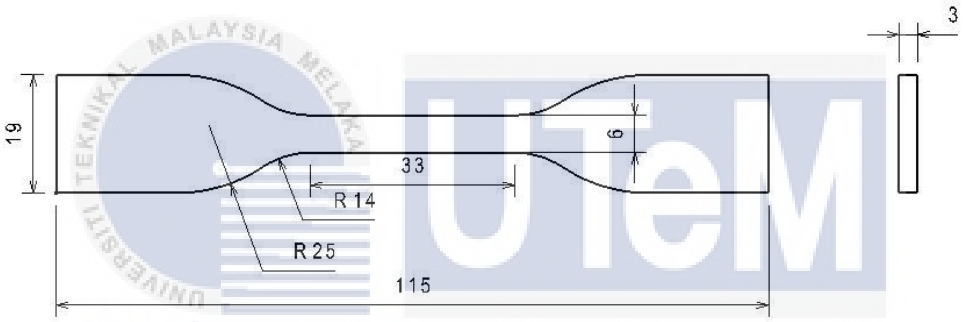

Figure 3.4: Dimension of tensile specimen based on the ASTM-D638 (Type IV) standard

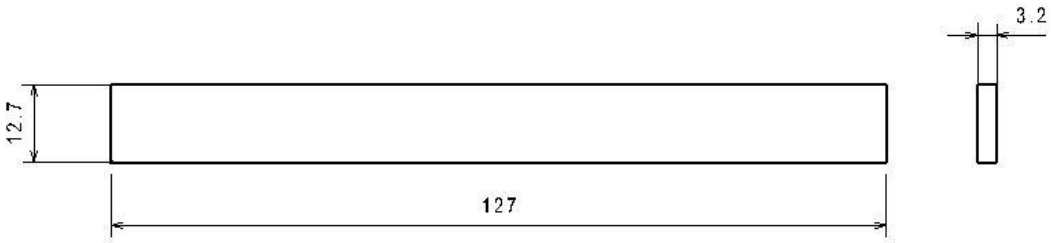

Figure 3.5: Dimension of flexural specimen based on the ASTM-D790 standard

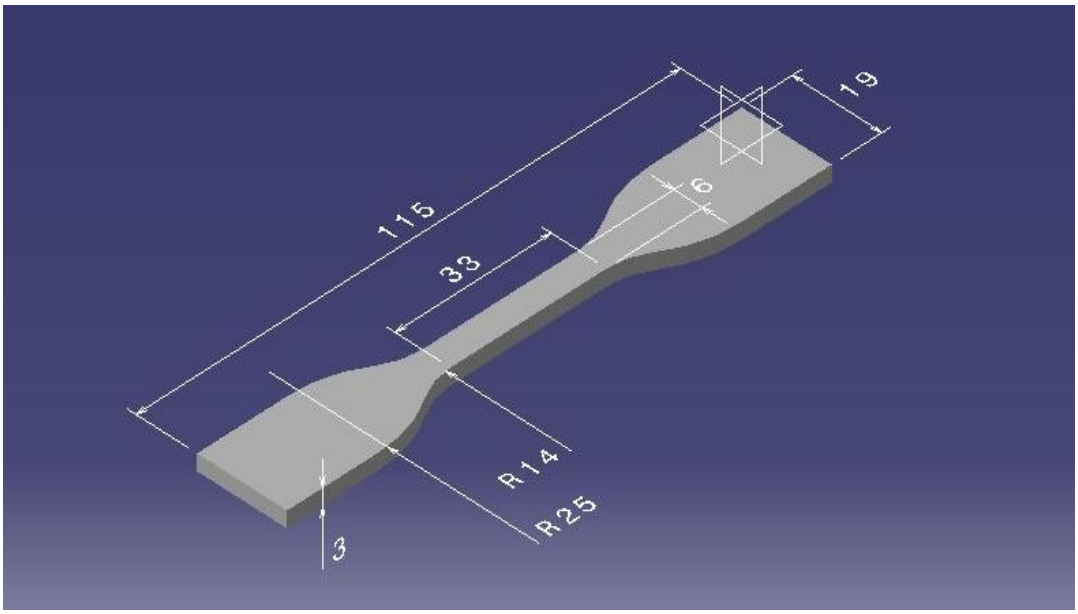

Figure 3.6: CAD model of ASTM-D638 (Type IV) standard

Figure 3.7: CAD model of ASTM-D790 standard

CAD is converted into STL files (stereolithography format) to proceed with the 3D printing process. Pre-printer is used to feed an STL file into a 3D slicer software, such as FlashPrint. The platforms are responsible for generating G-code, the native language of 3D printers. It also enables the opening and positioning of several models on a printing bed. Thus, several models can be printed simultaneously, allowing printing management easier for the workplace.

3.6 3D Printing

This study focuses on the FDM method of printing components using the FlashForge's Adventurer3 3D Printer, as shown in Figure 3.8. Adventurer3 is lightweight and portable because of its compressed and closed printed chamber. The most common defect in FDM, which is warping, can be avoided in the process since the machine is equipped with a heated bed up to 100°C. Adventurer3 comes with a heatable platform that can reach temperatures of 100°C. The build volume of FlashForge's Adventurer3 3D Printer is 150mm × 150mm × 150mm. Thus, the machine has a small build capacity making it ideal for printing specimens (ASTM D638-Type IV and ASTM D790). Figure 3.9 illustrates the setup for the 3D printing process in this study.

Figure 3.8: FlashForge's Adventurer3 3D Printer

Figure 3.9: 3D printing setup

3.6.1 Setting parameters

Many process parameters, such as the nozzle and build temperature, printing speed, and layer thickness, can be changed in most FDM systems. Few setting parameters have been set to follow during the printing process. The process parameters will remain the same for all three conditions of PLA filaments used. According to Valerga *et al.* (2018), a better mechanical strength is achieved at a higher printing temperature of 220°C. Initially, the printing temperature is set to 210°C, which corresponds to the suggested printing temperature for PLA by Hsueh *et al.* (2021), which is 190°C to 220°C. Also, every printer is different regarding print speed, and ideal settings can depend on the kind of printer to be used. However, PLA printing is typically fine at any speed from 40mm/s to 70mm/s, with the recommended speed of 60mm/s (Dwamena, 2020). A lower printer speed is more efficient to provide the better-finished output, with better quality results.

Besides, the effect of layer thicknesses is more readily visible when viewing print time and surface finish. Thinner layers provide a nice finish on the surface but more print time. Thicker layers contribute to bad finishing but quicker printing time. FDM can create the thinnest layers that can be done with standard equipment that are usually 0.05 thick. In addition, bed temperature is significant to allow materials to cool slower when extruded to prevent warping. It also gives added adhesion, meaning that the first layer holds well during printing, and the component is not released from the bed. Tyson (2018) stated 60°C as the best bed temperature for PLA. Other than that, it is recommended to use 100% as the filling percentage for a great result of mechanical resistance and quick printing (Alvarez *et al.*, 2016). The process parameters for FlashForge's Adventurer3 for printing the PLA specimens are set according to Table 3.2.

Table 3.2: Setting of process parameters for 3D printing

Parameter	Setting
1. Printing temperature (°C)	210
2. Bed temperature (°C)	60
3. Printing speed (mm/s)	60
4. Filling percentage (%)	100
5. Material	Polylactic acid (PLA)
6. Layer thickness (mm)	0.18 (default)

3.6.2 Number of specimens

The sample size is a crucial concern for analysis. Increasing the sample size offer more reliable mean values, detect outliers in a smaller sample that may distort the results, and give a lower error margin. In this study, 48 samples of specimens were printed using PLA filaments of three different conditions. Figure 3.10 shows three copies of the identical sample is printed at once with the same settings. The description of the type of PLA filaments and the number of specimens for the printing process is exemplified in Table 3.3.

Figure 3.10: 3D printed specimens

Table 3.3: The type of PLA filaments and number of specimens printed for the study

Condition of PLA Filaments		Number of Specimens	
		ASTM D638 Type IV standard	ASTM D790 standard
a) New PLA filament roll, brand new which acts as the reference.		3	3
b) Used PLA filament roll stored in the vacuum bag, with the desiccant.		3	3
c) Used PLA filament roll stored in open environment, exposed to a humidifier for variant of:	24 hours	3	3
	48 hours	3	3
	72 hours	3	3
	96 hours	3	3
	120 hours	3	3
	150 hours	3	3

3.7 Tensile Test

Tensile testing is carried out to achieve the first objective. This is one of the most popular mechanical testing methods to figure out how solid the object is and how long it can be extended until it fails. The test is used to assess ultimate tensile strength (UTS), yield strength, Young's modulus, strain hardening characteristics, and ductility. Shimadzu AGS-X universal testing machine is the equipment used to test the tensile properties in this study. The machine has a maximum load cell capacity of 20kN. The test speed is set to 5mm/min since Fahrenholz (2018) stated that it is the standard speed for the tensile test. The setup for the tensile test is illustrated in Figure 3.11.

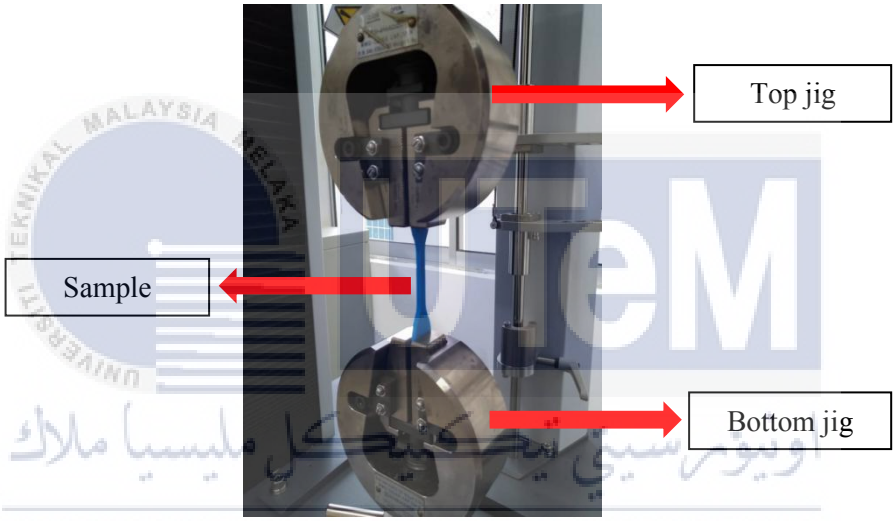

Figure 3.11: Tensile test setup

The maximum force, maximum stress, and maximum strain data were gathered and analyzed using the software "Trapezium-X" (Shimadzu Corp., Kyoto, Japan). The average tensile strength value for the three replications of each condition is calculated using Equation 3.1. The collected data is used to plot a stress-strain diagram to show the relationship between stress and strain in a material. Besides, the stress-strain curves between the three conditions were compared to determine the effect of humidity on the 3D printed parts. If the stress-strain curve changes when a PLA is subjected to humidity such as condition (c), it signifies that the properties of PLA have altered due to the humidity.

$$Average = \frac{Sum\ of\ tensile\ strength\ values}{Number\ of\ samples} \qquad (3.1)$$

3.8 Flexural Test

Flexural testing is carried out to achieve the second objective. This is one of the most popular mechanical testing methods to figure out how solid the object is and how long it can be extended until it fails. The test is used to assess ultimate tensile strength (UTS), yield strength, Young's modulus, strain hardening characteristics, and ductility. The flexural properties were also tested using a Shimadzu AGS-X universal testing machine in this study. The test speed is 50mm/min, as referred to Pugalendhi *et al.* (2019). Figure 3.12 illustrates the setup for the flexural test.

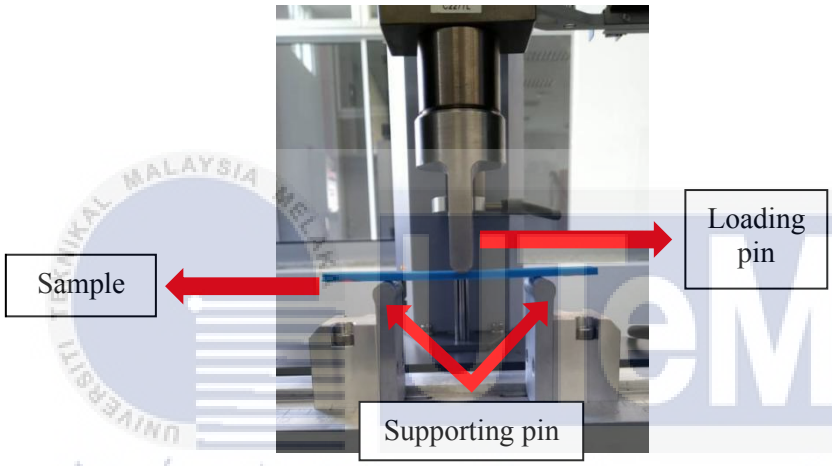

Figure 3.12: Flexural test setup

In addition, the span length and overhang determined the specimen length. When the span is short, the material modulus should be lower, and the span length should be 16 times the thickness. In this study, the span length = 3.2mm (thickness of sample) × 16 + 20% overhang = 61.44mm or approximately 62mm. Figure 3.13 displays an example of a specimen dimension for the flexural test by three-point bending.

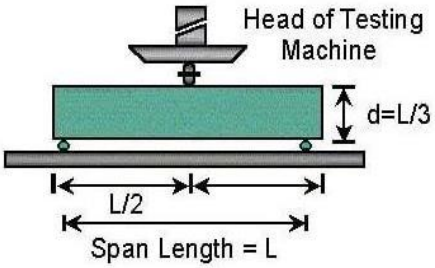

Figure 3.13: Example of a specimen dimension

The same data, such as maximum force, maximum stress, and maximum strain, were collected and examined using the software "Trapezium-X" (Shimadzu Corp., Kyoto, Japan). Equation 3.1 is also used to calculate the average flexural strength value for the three replications of each condition. Like the tensile test, the data gathered is used to create a stress-strain diagram that illustrates the relationship between stress and strain in a material. The stress-strain curves for the three conditions were then compared to see how humidity affected the 3Dprinted specimens. It is found that when a PLA is exposed to humidity, such as condition (c), the stress-strain curve changes, indicating that the PLA's characteristics have changed due to the humidity.

3.9 Sputter-coating

Sputter-coating is a physical vapour deposition method that coats a material with an extremely thin, functional layer of conductive metal, such as chromium, platinum, gold, or silver, to the sample. The sputtering-coat was utilised in this study for sample analysis so that the SEM images could be of the desired quality. PLA materials have surfaces that function as electron traps due to their non-conductive nature. The accumulation of electrons called charging on the surface resulted in extra-white areas on the sample that might affect image information. Thus, the conductive coating material functions as a route for the charged electrons to be withdrawn when sputter-coating is utilized, resulting in a high-quality SEM image. Figure 3.14 shows the difference in SEM images for (a) before sputter-coating and (b) after sputter-coating.

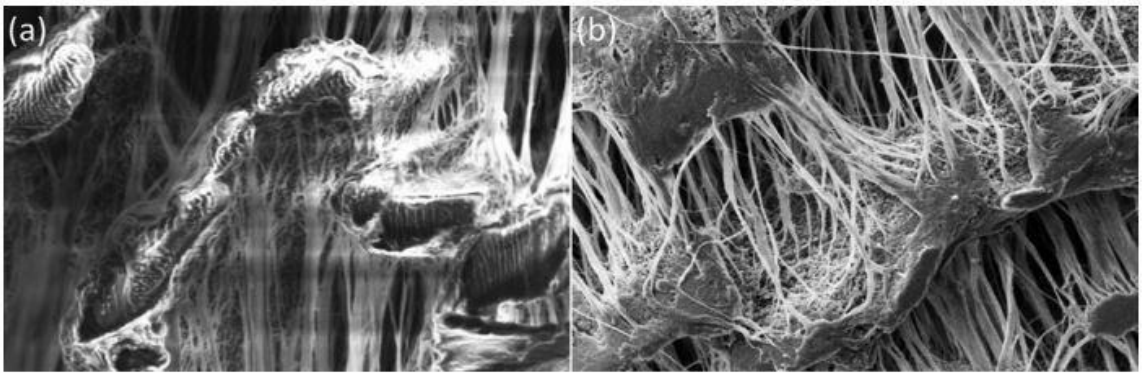

Figure 3.14: The difference in SEM images for (a) before sputter-coating and (b) after sputter-coating (Heu *et al.,* 2019)

Throughout this study, the fractured tensile samples with the closest maximum force value to the average value were used to analyse the microstructure using the scanning electron microscope (SEM). The total of eight samples was cut into 10 mm and then were sputter-coated with 10nm thick of gold-palladium using SC7620 Mini Sputter Coater machine as exhibited in Figure 3.14. Gold was chosen as a coater due to its high conductivity and tiny particle size, leading to a high-resolution image. It took three minutes to ensure the sample is thoroughly coated. The samples were kept in an airtight container after the coating process to prevent contamination.

Figure 3.15: SC7620 Mini Sputter Coater machine

3.10 Scanning Electron Microscopy (SEM) Analysis

This study conducted a microstructural analysis to gain detailed knowledge of the effects of humidity on the 3D printed specimens. After sputter-coating, the specimens were scanned using a scanning electron microscope for microstructure analysis. SEM visual inspection of a surface helps identify contaminates or undiscovered particles and the reason for failure and material interactions. SEM generates a range of signals at the surface of solid objects using a concentrated beam of high-energy electrons. Most SEM systems capture data across a particular region of the sample's surface and create a 2D image that depicts spatial changes in characteristics such as materials orientation, chemical characterization, and texture. In this study, surface images of the specimens were recorded at the secondary electron with a Carl Zeiss Evo 50 at 15.00kV accelerating voltage for 50x and 100x magnification power.

CHAPTER 4
RESULT AND DISCUSSION

This chapter presents the analysis of tensile strength, flexural strength, and SEM images of 3D printed PLA specimens from three different humidity conditions: (a) new PLA filament roll, which acts as the reference; (b) used PLA filament roll stored in the vacuum bag, with the addition of desiccant; (c) used PLA filament roll stored in an open environment, exposed to a humidifier for a variant of 24, 48, 72, 96, 120, and 150 hours. The stress-strain curve and SEM images for these three different humidity conditions are compared and discussed in this chapter.

4.1 Tensile Maximum Force and Maximum Stress Analysis

The average value of maximum force and maximum stress for each sample set was computed once the tensile test results were received. The findings are organised into groups based on the humidity conditions of PLA filaments used. Table 4.1 shows the average maximum force and maximum stress results of samples produced using:

a. New PLA filament roll, which acts as the reference.
b. Used PLA filament roll stored in the vacuum bag, with the addition of desiccant.
c. Used PLA filament roll stored in an open environment and exposed to a humidifier for variant of 24, 48, 72, 96, 120, and 150 hours.

Table 4.1: The average maximum force and maximum stress results for tensile test

Tensile test result for condition (a)		
Humidity Condition	**Maximum Force (Average) (N)**	**Maximum Stress (Average) (N/mm^2)**
New PLA filament roll, which acts as the reference	939.76	16.49
Tensile test result for condition (b)		
Humidity Condition	**Maximum Force (Average) (N)**	**Maximum Stress (Average) (N/mm^2)**
Used PLA filament roll stored in the vacuum bag, with an addition of desiccant	938.72	16.47
Tensile test result for condition (c)		
Humidity Condition	**Maximum Force (Average) (N)**	**Maximum Stress (Average) (N/mm^2)**
Humidified for 24 hours	860.29	15.09
Humidified for 48 hours	855.63	15.01
Humidified for 72 hours	852.78	14.96
Humidified for 96 hours	850.48	14.92
Humidified for 120 hours	848.69	14.88
Humidified for 150 hours	836.47	14.68

As shown in Table 4.1, the average maximum force and maximum stress values for each 3D printed object were different. For condition (a), where the samples were printed using the new PLA filament roll, the maximum average and maximum stress values were 939.76N and 16.49N/mm^2, respectively. Besides, the samples printed using the used PLA filament roll stored in the vacuum bag with the addition of desiccant recorded an average value of 938.72N for maximum force and 16.47N/mm^2 for maximum stress. These results revealed that the maximum force for the samples printed under condition (b) had a reduced average maximum force and maximum stress by 1.04N and 0.02N/mm^2 compared to the sample printed under condition (a). The average maximum force and maximum stress values for the 3D printed objects printed using the new PLA filament roll, which acts as a reference, were higher than 3D printed objects using the used PLA filament roll stored in the vacuum bag with the addition of desiccant. However, the result is only slightly different, which might be acceptable to say the dehumidifying agent is essential to help all 3D printer users control the humidity exposure of their used PLA filament.

Moreover, the average maximum force values for the 3D printed objects printed utilising condition (c) dropped from 860.29N to 836.47N as the humidity exposure was increased from 24 to 150 hours. The average maximum stress values also decreased from 15.09 N/mm^2 to 14.68 N/mm^2. Additionally, there was a difference of 103.29N in average maximum force between the 3D printed samples using new PLA filament roll and PLA filament humidified for 150 hours. Meanwhile, the average maximum stress value in those samples differed by 1.81N/mm^2. When the results of all of the humidity conditions were compared, the 3D printed object made with the PLA filament humidified for 150 hours had the lowest average maximum force and maximum stress values. In contrast, the 3D printed objects from the new PLA filament roll, which acts as the reference, had the most significant average maximum force and maximum stress values. These results indicated that humidity exposures had affected the maximum force and stress of the printed 3D objects.

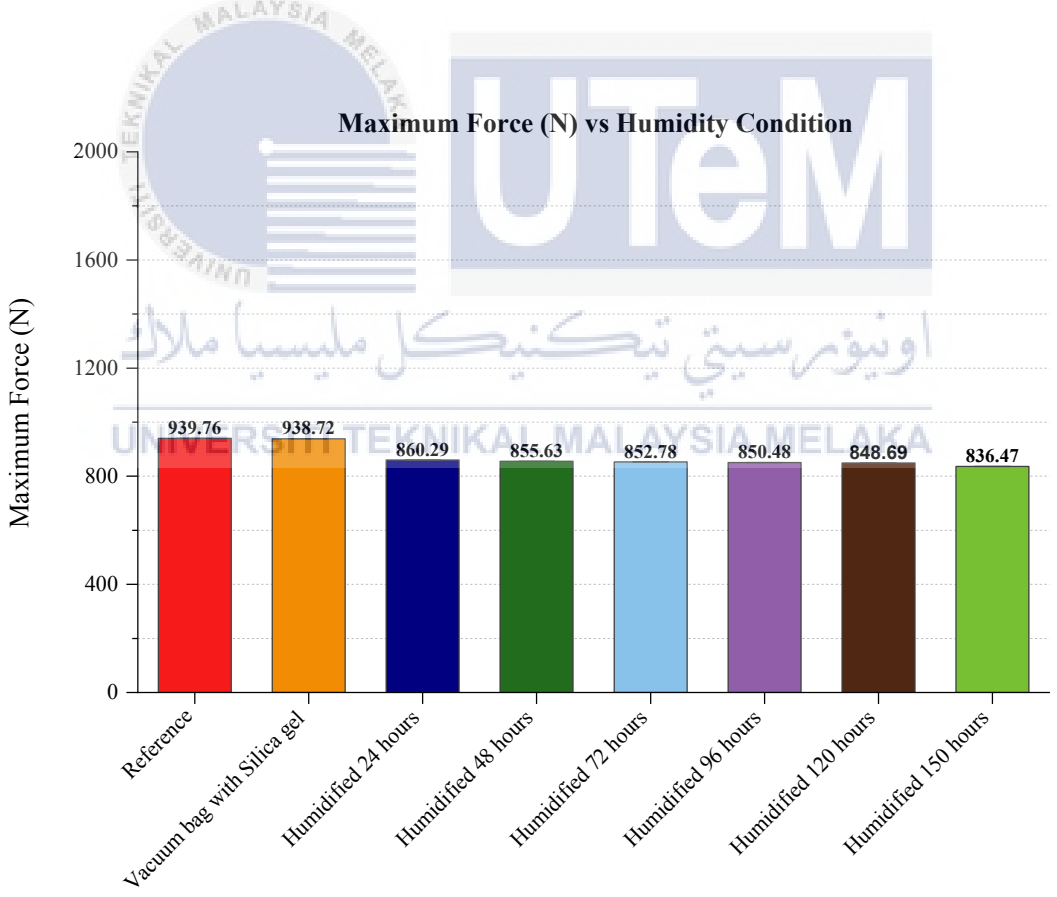

Figure 4.1: Tensile maximum force (N) plot for all conditions

Figure 4.1 shows a bar graph of the study. It depicts a comparison of the maximum forces for all conditions, where a strong correlation between the humidity and the maximum

force is observed. The graph shows that the sample printed with the new PLA filament roll (reference) had the most excellent maximum force value of 939.76N. The higher maximum force value resulted in higher tensile strength. As a result, the tensile strength of the sample produced using the new PLA filament roll (reference) is the highest among all samples.

On the other hand, the sample printed with the PLA filament humidified with the most extended hour for 150 hours had the lowest maximum force value of 836.47N. The tensile strength of the material will be the lowest since the maximum force value is the lowest. This finding indicates that when PLA filaments are exposed to humidity, the tensile strength of a 3D printed object gradually decreases.

4.2 Flexural Maximum Force and Maximum Stress Analysis

Once the flexural test results were received, each sample set's average maximum force and maximum stress value were evaluated. The results are classified depending on the humidity levels of the PLA filaments used. Table 4.2 displays the average maximum force and maximum stress results of samples produced using:

a. New PLA filament roll as the reference;
b. Used PLA filament roll stored in a vacuum bag with the addition of desiccant; and
c. Used PLA filament roll stored in an open environment, exposed to a humidifier for variant of 24, 48, 72, 96, 120, and 150 hours.

Table 4.2: The average maximum force and maximum stress results for flexural test

Flexural test result for condition (a)		
Humidity Condition	**Maximum Force (Average) (N)**	**Maximum Stress (Average) (N/mm^2)**
New PLA filament roll, which acts as the reference	127.16	90.93
Flexural test result for condition (b)		
Humidity Condition	**Maximum Force (Average) (N)**	**Maximum Stress (Average) (N/mm^2)**
Used PLA filament roll stored in the vacuum bag, with an addition of desiccant	115.23	82.41
Flexural test result for condition (c)		
Humidity Condition	**Maximum Force (Average) (N)**	**Maximum Stress (Average) (N/mm^2)**
Humidified for 24 hours	109.96	78.64
Humidified for 48 hours	108.51	77.60
Humidified for 72 hours	107.18	76.65
Humidified for 96 hours	104.66	74.85
Humidified for 120 hours	102.64	73.40
Humidified for 150 hours	101.55	72.62

The average maximum force and maximum stress values from the flexural test for each 3D printed object were also varied, as shown in Table 4.2. The samples produced with condition (a), the new PLA filament roll, had an average maximum force of 127.16N and maximum stress of 90.93N/mm^2. Furthermore, the samples printed using condition (c), the used PLA filament roll kept in a vacuum bag containing desiccant recorded an average value of 115.23N for maximum force and 82.41N/mm^2 for maximum stress. Compared to the samples printed under condition (b), the average maximum force and maximum stress decreased by 11.93N and 8.52N/mm^2, respectively, compared to the reference samples printed under condition (a). In this study, the flexural test's average maximum force and maximum stress values for 3D printed objects printed with new PLA filament roll, which served as a reference, were slightly higher than 3D printed objects printed with used PLA filament roll stored in the vacuum bag with desiccant.

The average maximum force values for the 3D printed objects decreased from 109.96N to 101.55N when the humidity exposure was extended from 24 to 150 hours in condition (c). The average maximum stress values fell from 78.64N/mm^2 to 72.62 N/mm^2 as well. Furthermore, the average maximum force between the 3D printed samples utilising new PLA filament roll and PLA filament humidified for 150 hours differed by 25.61N. Meanwhile, the maximum stress values in those samples differed by 6.02N/mm^2 on average. According to the results, the 3D printed object made using PLA filament humidified for 150 hours had the lowest average maximum force and maximum stress values for the flexural test. On the other hand, the average maximum force and maximum stress values for the 3D printed objects from the new PLA filament roll, which served as the reference, were the highest. These findings suggested that moisture exposure has influenced the maximum force and stress of 3D printed objects by lowering their value.

Figure 4.2 illustrates a bar graph from the study that compares the maximum forces to the humidity condition, where a strong correlation between the humidity and the maximum force is observed. Based on the plot, the samples printed with the new PLA filament roll (reference) had the highest maximum force value of 127.16N. The higher maximum force value resulted in higher flexural strength. Thus, the samples created with the new PLA filament roll (reference) had the maximum flexural strength. In addition, the samples printed with PLA filament that had been humidified for 150 hours had the lowest maximum force of 101.55N, resulting in the weakest flexural strength. This result consequently shows that the flexural strength of a printed 3D item is reduced when PLA filaments were exposed to humidity.

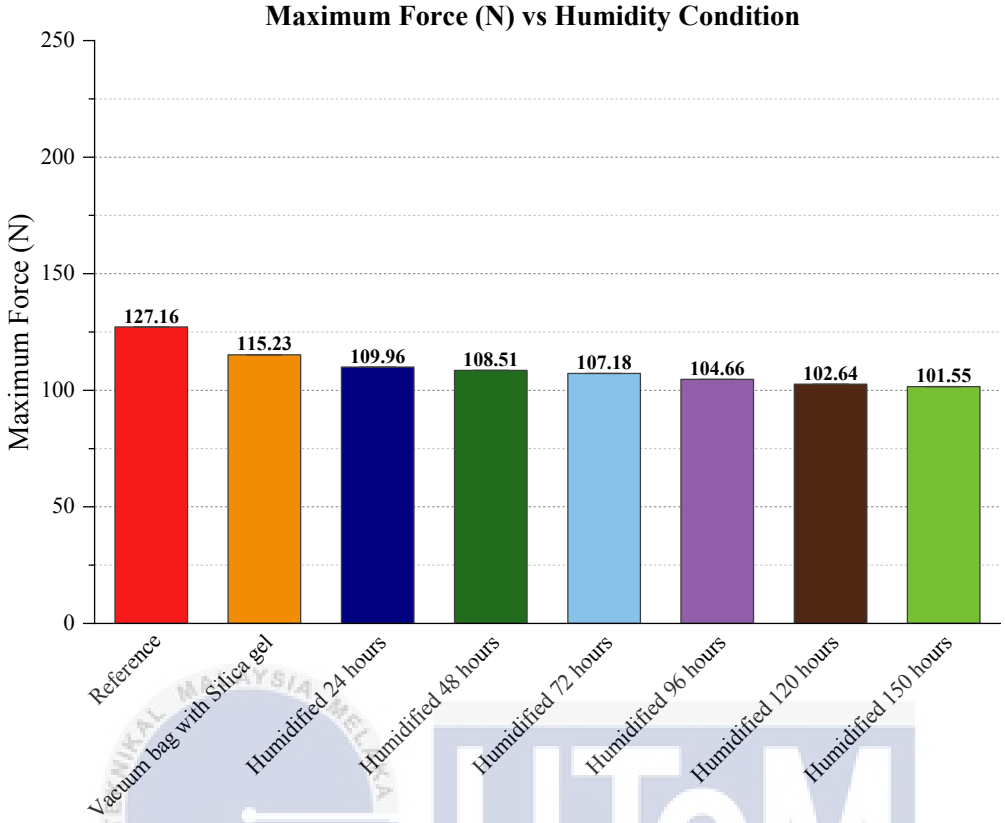

Figure 4.2: Flexural maximum force (N) plot for all conditions

4.3 Stress-strain Analysis

The stress-strain curve for material is used in engineering and materials science to show the connection between stress and strain. The stress-strain curve portrays how stress changes as strain rises. It is determined by gradually applying a load to a test coupon and monitoring the deformation. The shear stress and strain may be calculated. In this study, the ultimate tensile strength (UTS) and ultimate flexural strength (UFS) were analysed to determine the highest stress that 3D printed objects can withstand before breaking while being stretched or pulled after being produced under various humidity conditions of PLA filaments. Besides, Equation 4.1 and Equation 4.2 were used to determine the stress and strain values based on the tensile test results. All of the data were plotted onto the graph when the calculation was completed.

$$\sigma = \frac{P}{A} \qquad (4.1)$$

Where σ is normal stress

P is axial force

A is cross sectional area

$$\varepsilon = \frac{\Delta L}{L_0} \qquad (4.2)$$

Where ε is a strain,

ΔL is total elongation

L_0 is original length

4.3.1 Tensile-stress-strain Analysis

The stress-strain curve of the tensile test result is shown in Figure 4.3. The stress-strain curves showed that the tensile strength is affected by the humidity condition of the PLA filament. The UTS of the 3D printed object made using PLA filament humidified for 150 hours was the lowest. Meanwhile, the 3D-printed item with the new PLA filament served as a reference had the greatest UTS. Furthermore, the strain value of the necking area, which represents the strain value from UTS to fracture, varies depending on humidity level; however, the lengths were unequal. As demonstrated in Figure 4.3, the fracture strain of 3D printed objects printed with humidified PLA filament for 150 hours was greater than that of 3D printed objects printed with new PLA filament, which acts as a reference.

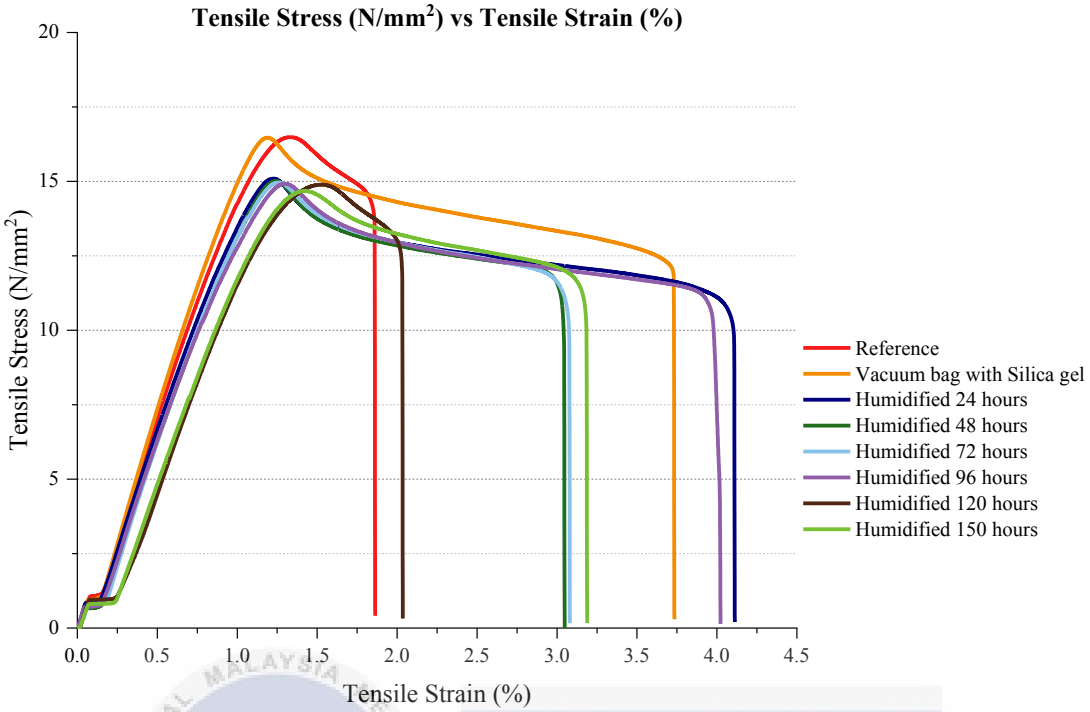

Figure 4.3: Stress-strain curve for tensile test

As the PLA filaments were exposed to humidity, there were high chances that the filament will absorb moisture from the air. The rise of moisture level is equivalent to the decrease in stress and the increase in strain resulting from hydrogen bonding between polymer chains. Back to the fundamental of material, the water molecules have penetrated the structure of PLA as moisture is absorbed. The water molecules function as plasticizers, forming hydrogen bonds between the C-O and N-H groups, allowing polymer chains to move freely. This has permitted the movement of the polymer chains to increase.

Moreover, humidity's plasticizing impact on PLA enhanced its deformability while reducing its rigidity. As a result, the PLA became easier to bend, resulting in improved capacity to stretch plastically at room temperature without breaking. This behaviour clarifies why the fracture strain increases as the stress decrease.

4.3.2 Flexural-stress-strain Analysis

Figure 4.4 shows the stress-strain curve of the flexural test result, which revealed that the humidity state of the PLA filament impacted flexural strength. The 3D printed object with the lowest UFS was produced with PLA filament humidified for 150 hours. Meanwhile, the 3D printed object using the new PLA filament (reference) had the highest UFS. The fracture strain of 3D printed objects using PLA filament humidified for 150 hours is lower than 3D printed objects from new PLA filament roll (reference) and used PLA filament roll stored in the vacuum bag, with the desiccant. Thus, this study showed that the ultimate flexural strength increases while decreasing the fracture strain as humidity increases.

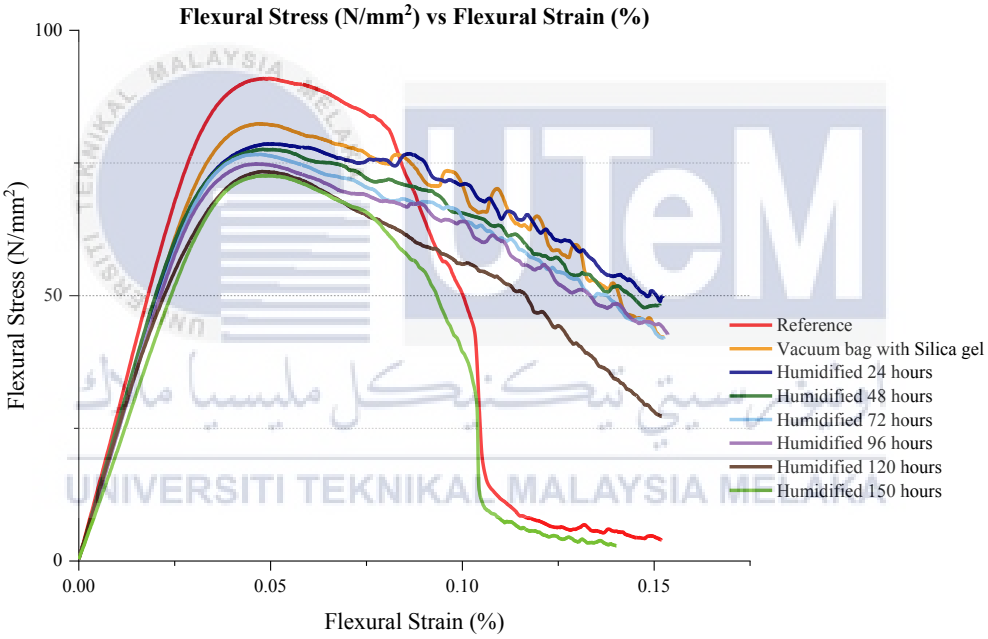

Figure 4.4: Stress-strain curve for flexural test

4.4 Microstructure Analysis

The fractured surface of each sample was examined using a scanning electron microscope (SEM) with a voltage of 15.00kV and magnification ranges of 50x and 100x. The picture seen is the gap between layers by layer that emerges as PLA materials are extruded from an FDM nozzle. According to the tensile and flexural test results, the 3D printed objects utilising the new PLA filament have the highest maximum force value

compared to other humidity conditions of PLA filament. Microstructure analysis helped determine why the tensile and flexural stress and strain values of the 3D printed items differed.

The length of the interlayer gaps between each sample was determined using ImageJ software after the SEM images were captured. The first step of using the ImageJ software is to set the scale. Therefore, the same scale was used to measure the length of the interlayer gap for the SEM images. Figures 4.5-4.7 show the measured interlayer gap of the 3D printed objects. In the meantime, the findings of ImageJ software for the length of the interlayer gap were recorded in Table 4.3.

Figure 4.5: The measured interlayer gap of the 3D printed objects using new PLA filament (reference)

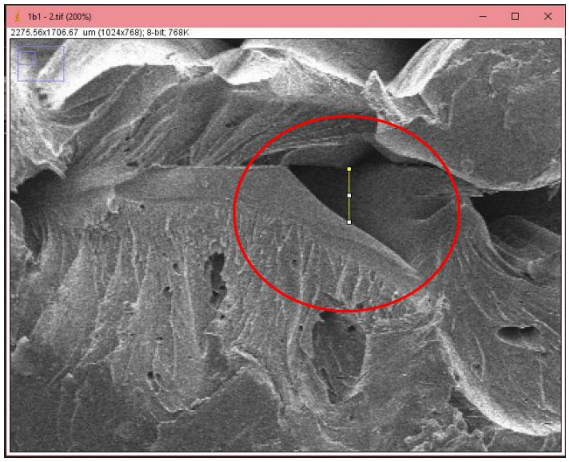

Figure 4.6: The measured interlayer gap of the 3D printed objects using used PLA filament stored in vacuum bag with addition of desiccant

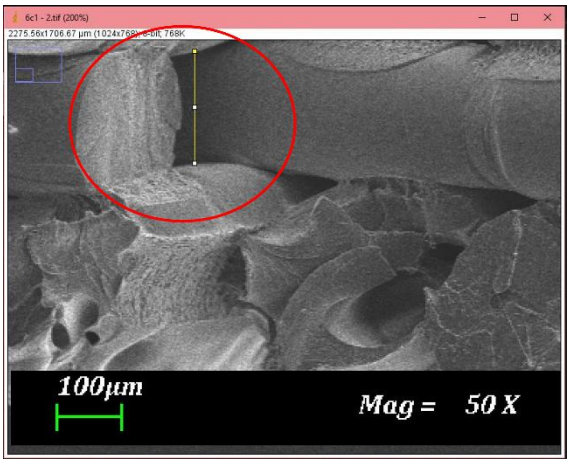

Figure 4.7: The measured interlayer gap of the 3D printed objects using PLA filament humidified for 150 hours

Table 4.3: The findings of ImageJ software for the length of the interlayer gap

Sample	Length, L (mm)			Average (mm)	Angle (°)
	L_1	L_2	L_3		
New PLA filament (Reference)	51.11	56.67	67.78	58.52	-90
Vacuum bag with desiccant	82.22	76.67	82.22	80.37	-90
Humidified for 150 hours	171.11	177.78	173.33	174.07	-90

Based on Table 4.3, the length of the interlayer gap in the SEM image for the 3D sample printed using PLA filament humidified for 150 hours was the longest. The length of the interlayer gap in the SEM image for the 3D sample printed using the new PLA filament (reference) was the shortest. Humidity has expanded the interlayer gap, which might enhance the fracture strain due to the increased number of polymer chains. Samples printed using filament humidified for 150 hours have a more significant gap between the interlayer than other samples, resulting in low tensile and flexural strength. Therefore, this study concludes that the larger the interlayer gap, the lower the tensile and flexural strength.

CHAPTER 5
CONCLUSION AND RECOMMENDATION

The findings of the effects of humidity on the mechanical properties and microstructure of 3D printed PLA filament are summarised in this chapter. Also, this chapter includes recommendations for future study.

5.1 Conclusion

In this study, the effects of humidity on the mechanical properties and microstructure of 3D printed PLA filament were investigated. The expected influence of humidity on the tensile and flexural strength was evident. The following are the conclusion that can be drawn from this study:

(a) The first objective to analyse 3D specimens fabricated using the non-exposed and moisture-exposed PLA filaments was achieved. The tensile strength decreases as humidity increases. Besides, the presence of moisture causes a plasticizing effect of the polymer, which increases the fracture strain.

(b) As for the second objective, which is to examine the flexural strength of the 3D parts produced from the non-exposed and moisture-exposed PLA filaments, was accomplished. The flexural strength reduces as humidity increases.

(c) Moreover, the third objective was also succeeded, and microstructure analysis verified the acquired tensile and flexural results since longer interlayer gaps were found in the weakest sample. The expansion of the interlayer gap caused by humidity results in low tensile and flexural strength of the 3D printed objects.

(d) However, the used PLA filament stored in a vacuum bag with some dehumidifying agents shows an equivalent tensile strength with the reference specimen. In conclusion, humidity influences the mechanical properties and should be controlled for a good printing quality of PLA parts.

5.2 Recommendation

In terms of future study, the following recommendations are suggested:

(a) This study can be improved by using a proper humidity device such as a dry cabinet box with controllable humidity to control the humidity level.

(b) PLA filaments should be stored in a drying cabinet with controllable humidity. Otherwise, all 3D printing users are advised to permanently seal the used PLA filament in a vacuum bag with some dehumidifying agents.

(c) The humidity level in PLA filaments needs to be measured before printing to ensure good results. It is recommended to set up a real-time humidity measurement device upon the 3D printing process to control the humidity factor.

(d) Regular maintenance for the 3D printing machines and drying cabinet is needed to avoid defects. If there are many defects product produced, more plastic will end up in landfills and causing unsustainable 3D printing.

5.3 Sustainability Element

The material utilised in this study was biodegradable PLA filament. It is one of the most common materials that fulfil the economically practical manufacturing of non-petroleum plastic. Ultimately nature degrades when exposed to the environment. PLA also has one of the recyclable materials. Therefore, the printed PLA parts can be recycled through the correct procedure to ensure their sustainability.

5.4 Lifelong Learning Element

The feature of lifelong learning is defined as a form of self-directed education that focuses on personal growth. Lifelong learning is also described as the formation of human capacity via a process that continually supports and promotes the acquisition of all the knowledge, values, abilities, and understanding necessary throughout life and can be applied to all the tasks. This study will aid in the development of a better understanding of additive manufacturing (AM) technology.

5.5 Complexity Element

The humidity level was one of the study's complexities since it is difficult to control. Initially, the moisture metre was used to measure the humidity level in the filament, but it was unable to detect any measurement, despite the manufacturer's claim that it could be used to do so. Besides, the humidifier's water must be changed on a frequent basis because it only lasts for 2-3 hours. Due to the limited availability of laboratories during the Covid-19 pandemic epidemic, only the fractured samples with the closest maximum force value to the average value were selected for microstructure examination using the scanning electron microscope (SEM). Furthermore, the FTIR test and density test (Archimedes Principle) were planned to be included in this study to explore hydrogen bonding between polymer chains and to determine if density is affected by humidity because density is connected to porosity. However, owing to the pandemic outbreak, laboratory utilisation has been restricted, thus neither test can be performed.

REFERENCES

Chola. (2017, March 09). PLA Filament Moisture Study: Effect of Moisture on 3D Printing Filament Properties. Retrieved December 28, 2020, from https://3dprinterchat.com/pla-filament-moisture-study/

Álvarez, K., Lagos, R. F., & Aizpun, M. (2016). Investigating the influence of infill percentage on the mechanical properties of fused deposition modelled abs parts. *Ingeniería E Investigación, 36*(3), 110. doi:10.15446/ing.investig.v36n3.56610

Attaran, M. (2017). The rise of 3-D printing: The advantages of additive manufacturing over traditional manufacturing. *Business Horizons, 60*(5), 677-688. doi: 10.1016/j.bushor.2017.05.011

Avinc, O., & Khoddami, A. (2009). Overview of Poly(lactic acid) (PLA) Fibre. *Fibre Chemistry, 41*(6), 391-401. doi:10.1007/s10692-010-9213-z

Avinc, O., & Khoddami, A. (2016). Overview of Poly (lactic acid) (PLA) Fibre: Part I: Production, Properties, Performance, Environmental Impact, and End-use Applications of Poly (lactic acid) Fibres. *Fibre Chemistry,* (6).

Bhuvanesh Kumar, M., & Sathiya, P. (2020). Methods and materials for additive manufacturing: A critical review on advancements and challenges. *Thin-Walled Structures, 159*, 107228. doi:10.1016/j.tws.2020.107228

Dey, A., & Yodo, N. (2019). A Systematic Survey of FDM Process Parameter Optimization and Their Influence on Part Characteristics. *Journal of Manufacturing and Materials Processing, 3*(3), 64. doi:10.3390/jmmp3030064

Dhinesh, S., Arun, P. S., Senthil, K. K., & Megalingam, A. (2020). Study on flexural and tensile behavior OF PLA, ABS And PLA-ABS materials. *Materials Today: Proceedings, 45*, 1175-1180. doi:10.1016/j.matpr.2020.03.546

Dugan, J. S. (2001). Novel Properties of PLA Fibers. *International Nonwovens Journal*, *os-10*(3), 1558925001OS – 01. https://doi.org/10.1177/1558925001os-01000308

Durga Prasada Rao, V., Rajiv, P., & Navya Geethika, V. (2019). Effect of fused deposition modelling (FDM) process parameters on tensile strength of carbon fibre PLA. *2nd International Conference on Applied Sciences and Technology (ICAST-2019): Materials Science,* 24-25 October 2019, Bali, Indonesia.

Dwamena, M. (2020, December 21). PLA 3D printing speed & temperature - which is best? Retrieved August 29, 2021, from https://3dprinterly.com/pla-3d-printing-speed-temperature-which-is-best/

Fahrenholz, H. (2018). Plastics: Determinataion of tensile properties. *The 2012 version of ISO 527*, 1-27.

Farah, S., Anderson, D. G., & Langer, R. (2016). Physical and mechanical properties of PLA, and their functions in widespread applications — A comprehensive review. *Advanced Drug Delivery Reviews*, *107*, 367–392. https://doi.org/10.1016/j.addr.2016.06.012

Goldstein. (2012). Scanning Electron Microscopes. *Cell Biology. Third Edition*, 54-89.

Gupta, B., Revagade, N., & Hilborn, J. (2007a). Poly(lactic acid) fiber: An overview. *Progress in Polymer Science*, *32*(4), 455–482. https://doi.org/10.1016/j.progpolymsci.2007.01.005

Gupta, B., Revagade, N., & Hilborn, J. (2007b). Poly(lactic acid) fiber: An overview. *Progress in Polymer Science*, *32*(4), 455–482. https://doi.org/10.1016/j.progpolymsci.2007.01.005

Hamid, R. A., Kasim, M. S., Izamshah, R., Hafiz, M. S. A., & Muhamad, W. N. A. W. (2019). Effect of process parameters on mechanical properties of PLA parts for a low cost 3D printing. 1–11.

Haryńska, A., Carayon, I., Kosmela, P., Szeliski, K., Łapiński, M., Pokrywczyńska, M., . . . Janik, H. (2020). A comprehensive evaluation of flexible FDM/FFF 3D printing filament as a potential material in medical application. *European Polymer Journal, 138*, 109958. doi:10.1016/j.eurpolymj.2020.109958

Henton, D. E., Gruber, P., Lunt, J., & Randall, J. (2005). Polylactic Acid Technology. *Natural Fibers, Biopolymers, and Biocomposites,* 527-578.

Heu, R., Shahbazmohamadi, S., Yorston, J., & Capeder, P. (2019). Target material selection for sputter coating of sem samples. *Microscopy Today*, *27*(4), 32–36. https://doi.org/10.1017/s1551929519000610

Hsueh, M., Lai, C., Wang, S., Zeng, Y., Hsieh, C., Pan, C., & Huang, W. (2021). Effect of Printing parameters on the thermal and mechanical properties Of 3d-printed PLA AND Petg, using fused deposition modeling. *Polymers, 13*(11), 1758. doi:10.3390/polym13111758

Jamshidian, M., Tehrany, E. A., Imran, M., Jacquot, M., & Desobry, S. (2010). Poly-Lactic Acid: Production, Applications, Nanocomposites, and Release Studies. *Comprehensive Reviews in Food Science and Food Safety*, *9*(5), 552–571. https://doi.org/10.1111/j.1541-4337.2010.00126.x

Jo, W., Kwon, O., & Moon, M. (2018). Investigation of influence of heat treatment on mechanical strength of FDM printed 3D objects. *Rapid Prototyping Journal, 24*(3), 637-644. doi:10.1108/rpj-06-2017-0131

Kakanuru, P., & Pochiraju, K. (2020). Moisture Ingress and Degradation of Additively Manufactured PLA, ABS and PLA/SiC Composite Parts. *Additive Manufacturing*, *36*, 101529. https://doi.org/10.1016/j.addma.2020.101529

Kariz, M., Sernek, M., & Kuzman, M. K. (2018). Effect of Humidity on 3d-Printed Specimens from Wood-PLA Filaments. *Wood Research, 63*(5), 917-922.

Karthik, T. (2004). Novel properties of PLA fibers. *Synthetic Fibres*, *33*(4), 5–10. https://doi.org/10.1177/1558925001os-01000308

Kumar, M. B., & Sathiya, P. (2020). Methods and materials for additive manufacturing: A critical review on advancements and challenges. *Thin-Walled Structures,* 107228. doi: 10.1016/j.tws.2020.107228

Kwon, S., Lee, S., Kim, Y., Oh, Y., Lee, S., Kim, J., & Kwon, J. (2020). A Filament Supply System Capable of Remote Monitoring and Automatic Humidity Control for 3D Printer. *Journal of Sensors, 2020*, 1-10. doi:10.1155/2020/8846466

Lasprilla, A. J. R., Martinez, G. A. R., Lunelli, B. H., Jardini, A. L., & Filho, R. M. (2012). Poly-lactic acid synthesis for application in biomedical devices — A review. *Biotechnology Advances*, *30*(1), 321–328. https://doi.org/10.1016/j.biotechadv.2011.06.019

Lesaffre, N., Bellayer, S., Vezin, H., Fontaine, G., Jimenez, M., & Bourbigot, S. (2017). Recent advances on the ageing of flame retarded PLA: Effect of UV-light and/or relative humidity. *Polymer Degradation and Stability, 139*, 143-164. doi: 10.1016/j.polymdegradstab.2017.04.007

Lewis, C. M., & Chambers, D. J. (2020). Humidity. *Anaesthesia and Intensive Care Medicine,* 1-4. doi: 10.1016/j.mpaic.2020.11.011

Lim, L.-T., Auras, R., & Rubino, M. (2008). Processing technologies for poly(lactic acid). *Progress in Polymer Science*, *33*(8), 820–852. https://doi.org/10.1016/j.progpolymsci.2008.05.004

Liu, C., Jiang, P., & Jiang, W. (2017). Embedded-web-based remote control for RepRap-based open-source 3D printers. *IECON 2017 - 43rd Annual Conference of the IEEE Industrial Electronics Society*. doi:10.1109/iecon.2017.8216573

Mallick, S., Ahmad, Z., Touati, F., Bhadra, J., Shakoor, R., & Al-Thani, N. (2018). PLA-TiO2 nanocomposites: Thermal, morphological, structural, and humidity sensing

properties. *Ceramics International, 44*(14), 16507-16513. doi: 10.1016/j.ceramint.2018.06.068

Masood, S. H. (1996). Intelligent rapid prototyping with fused deposition modelling. *Rapid Prototyping Journal, 2*(1), 24-33. doi:10.1108/13552549610109054

Mazurchevici, A. D., Nedelcu, D., & Popa, R. (2020). Additive manufacturing of composite materials by FDM technology: A review. *Indian Journal of Engineering and Materials Sciences, 27*(2), 179-192.

Mohamed, O. A., Masood, S. H., & Bhowmik, J. L. (2015). Optimization of fused deposition modeling process parameters: A review of current research and future prospects. *Advances in Manufacturing, 3*(1), 42-53. doi:10.1007/s40436-014-0097-7

Murariu, M., & Dubois, P. (2016). PLA composites: From production to properties. *Advanced Drug Delivery Reviews*, *107*, 17–46. https://doi.org/10.1016/j.addr.2016.04.003

Pugalendhi, A., Ranganathan, R., & Ganesan, S. (2019). Impact of process parameters on mechanical behaviour in multi-material jetting. *Materials Today: Proceedings*. doi:10.1016/j.matpr.2019.12.106

Raj, S. A., Muthukumaran, E., & Jayakrishna, K. (2018). A case study of 3d printed pla and its mechanical properties. *Materials Today: Proceedings, 5*(5), 11219-11226. doi:10.1016/j.matpr.2018.01.146

Raza, S. M., & Singh, D. (2020). Experimental Investigation on Filament Extrusion using recycled materials.

Saba, N., Jawaid, M., & Sultan, M. (2018). An overview of mechanical and physical testing of composite materials. *Mechanical and Physical Testing of Biocomposites, Fibre-Reinforced Composites and Hybrid Composites,* 1-12.

Singh, S., Rajeshkannan, A., Feroz, S., & Jeevanantham, A. K. (2020). Effect of Normalizing on the Tensile Strength, Shrinkage and Surface Roughness of PLA Plastic. *International Conference on Advances in Materials and Manufacturing Applications, IConAMMA 2018*, 16- 18 August 2018, Bangalore, India. 3–7.

Tamez, M. B., & Taha, I. (2021). A review of additive manufacturing technologies and markets for thermosetting resins and their potential for carbon fiber integration. *Additive Manufacturing, 37*, 101748. doi: 10.1016/j.addma.2020.101748

Titone, V., Correnti, A., & La Mantia, F. P. (2021). Effect of moisture content on the processing and mechanical properties of a biodegradable polyester. *Polymers, 13*(10), 1616. doi:10.3390/polym13101616

Tyson, M. (2018, May 21). Advanced guide to printing PLA Filament. Retrieved August 29, 2021, from https://www.3dprintingsolutions.com.au/User-Guides/how-to-3d-print-pla-filament

Valerga, A., Batista, M., Salguero, J., & Girot, F. (2018). Influence of PLA Filament Conditions on Characteristics of FDM Parts. *Materials, 11*(8), 1322. doi:10.3390/ma11081322

Wang, X., Jiang, M., Zhou, Z., Gou, J., & Hui, D. (2017). 3D printing of polymer matrix composites: A review and prospective. *Composites Part B: Engineering, 110*, 442-458. doi: 10.1016/j.compositesb.2016.11.034

What Effect Does Moisture Have on 3D Printer Filament Storage? (And how to fix it). (2020, October 19). Retrieved December 28, 2020, from https://blog.gotopac.com/2018/03/01/how-3d-printer-filament-storage-cabinets-instantly-improve-3d-print-part-quality/

Xiao, Lin & Wang, Bo & Yang, Guang & Gauthier, Mario. (2012). Poly(Lactic Acid)-Based Biomaterials: Synthesis, Modification and Applications. 10.5772/23927.

Yadav, P., Angajala, D. K., Singhal, I., Sahai, A., & Sharma, R. S. (2020). Evaluating mechanical strength of three dimensional printed PLA parts by free form fabrication. *International Mechanical Engineering Congress 2019: Materials Science*, 29 November – 1 December 2019, Tiruchirappalli, India. 3–7.

Yu, Y. (2012). *The effect of moisture absorption on the physical properties of polyurethane shape memory polymer foams* (Master's thesis, 2012). College Station, TX: Texas A & M University.

Zaldivar, R., Mclouth, T., Ferrelli, G., Patel, D., Hopkins, A., & Witkin, D. (2018). Effect of initial filament moisture content on the microstructure and mechanical performance Of ULTEM® 9085 3D printed parts. *Additive Manufacturing, 24*, 457-466. doi:10.1016/j.addma.2018.10.022

Zhang, X., Fan, W., & Liu, T. (2020). Fused deposition modeling 3D printing of polyamide-based composites and its applications. *Composites Communications, 21*, 100413. doi: 10.1016/j.coco.2020.100413

APPENDICES

A Gantt Chart of FYP 1

No	Activities	SEMESTER 1 (WEEK)														
		1	2	3	4	5	6	7	8	9	10	11	12	13	14	15
1	PSM Title Registration								MID SEMESTER BREAK							
2	First Briefing of Title															
3	Searching for related journals/articles															
4	Chapter 1 Introduction															
5	Chapter 2 Literature Review															
6	Chapter 3 Methodology															
7	Abstract															
8	Table of Content															
9	References															
10	Logbook submission															
11	Online Presentation															
12	FYP 1 Report Submission															